Ocean Spectral Data Analysis/Assimilation

-Optimal Spectral Decomposition (OSD) Method-

Peter C Chu
Department of Oceanography
Naval Postgraduate School

Atmospheric and Oceanic Sciences, UCLA, Los Angeles, 21 April 2016

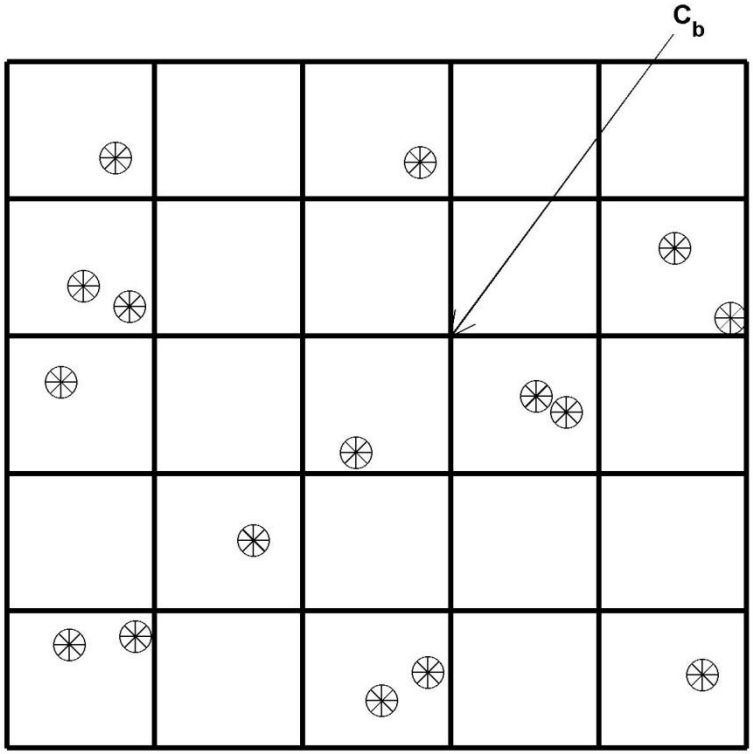
Outline

- (1) Introduction
- (2) Optimal Spectral Decomposition
- (3) Synoptic Monthly Gridded World Ocean Database (WOD) → Two Types of El Nino
- (4) Mid-Depth Rossby Wave Propagation
- (5) Conclusions

References

- Chu, P.C., C.W. Fan, and T. Margolina, 2016: Ocean spectral data assimilation without background error covariance matrix. *Ocean Dynamics*, in press.
- Chu, P.C., R.T. Tokmakian, C.W. Fan, and C.L. Sun, 2015: Optimal spectral decomposition (OSD) for ocean data assimilation. *Journal of Atmospheric and Oceanic Technology*, **32**, 828-841.
- Chu, P.C., 2011: Global upper ocean heat content and climate variability. *Ocean Dynamics*, **61** (8), 1189-1204.
- Chu, P.C., L.M. Ivanov, O.V. Melnichenko, and N.C. Wells, 2007: Long baroclinic Rossby waves in the tropical North Atlantic observed from profiling floats. *Journal of Geophysical Research*, **112**, C05032, doi:10.1029/2006JC003698.
- Chu, P.C., L.M. Ivanov, T.P. Korzhova, T.M. Margolina, and O.M. Melnichenko, 2003: Analysis of sparse and noisy ocean current data using flow decomposition. Part 2: Application to Eulerian and Lagrangian data. *Journal of Atmospheric and Oceanic Technology*, **20**, 492-512.
- Chu, P.C., L.M. Ivanov, T.P. Korzhova, T.M. Margolina, and O.M. Melnichenko, 2003: Analysis of sparse and noisy ocean current data using flow decomposition. Part 1: Theory. *Journal of Atmospheric and Oceanic Technology*, **20** (4), 478-491.

(1) Introduction



Ocean data assimilation with $\boldsymbol{c}_b$ located at the grid points, and $\boldsymbol{c}_o$ located at the points '*'. The ocean data assimilation is to convert the innovation, $\boldsymbol{d} = \boldsymbol{c}_o - \mathbf{H}\boldsymbol{c}_b$, from the observational points to the grid points.

Assimilated Variable $\mathbf{c}(\mathbf{x}, z, t)$

$\mathbf{c}_t \rightarrow$ "true"

$\mathbf{c}_a \rightarrow$ analysis (assimilated)

$\mathbf{c}_b \rightarrow$ background (modeled)

$(\mathbf{c}_t, \mathbf{c}_a, \mathbf{c}_b) \rightarrow$ grid points $\rightarrow$ $\mathbf{r}_n \rightarrow$ total N

$\mathbf{c}_o \rightarrow$ Observation $\rightarrow$ Obs points $\rightarrow$ $\mathbf{r}^{(m)}$

$\rightarrow$ total M

Traditional Ocean Data Assimilation Schemes

- Optimal Interpolation (OI)
- Kalman Filter
- Variational Methods

Data Assimilation

$$\mathbf{c}_a = \mathbf{c}_b + \mathbf{W}\mathbf{d}$$

Innovation → $\mathbf{d} = \mathbf{c}_o - \mathbf{H}\mathbf{c}_b$

Various ways → **W** – Weight Matrix
→ Different Data Assimilation Schemes

H =$[h_{mn}]$ → the $M \times N$ linear observation operator matrix

W → Depends on **B**, **R**

B → Background Error Covariance Matrix

R → observational error covariance matrix (usually assumed given)

Background Error Covariance Matrix B & Observational Error Covariance Matrix R

$$\boldsymbol{\varepsilon}_a = \mathbf{c}_a - \mathbf{c}_t, \quad \boldsymbol{\varepsilon}_o \equiv \mathbf{H}^T \mathbf{c}_o - \mathbf{c}_t$$

$$E^2 = \left\langle \boldsymbol{\varepsilon}_a^T \boldsymbol{\varepsilon}_a \right\rangle \rightarrow \min$$

$$\partial E^2 / \partial w_{nm} = 0$$

- Optimal Interpolation (OI)

$$\mathbf{W} = \mathbf{B}\mathbf{H}^T (\mathbf{R} + \mathbf{H}\mathbf{B}\mathbf{H}^T)^{-1}$$

- Kalman Filter (KF)

$$\mathbf{W}_i = \mathbf{B}^f(t_i)\mathbf{H}^T [\mathbf{R}_i + \mathbf{H}_i \mathbf{B}^f(t_i)\mathbf{H}^T]^{-1}$$

- Variational Method

$$\mathbf{W} = (\mathbf{B}^{-1} + \mathbf{H}^T \mathbf{R}^{-1} \mathbf{H})^{-1} \mathbf{H}^T \mathbf{R}^{-1}$$

Data Assimilation Equation (OI/KF)

$$\mathbf{c}_a = \mathbf{c}_b + \mathbf{B}\mathbf{H}^T(\mathbf{H}\mathbf{B}\mathbf{H}^T + \mathbf{R})^{-1}\mathbf{d}$$

→ Dependent on the selection of

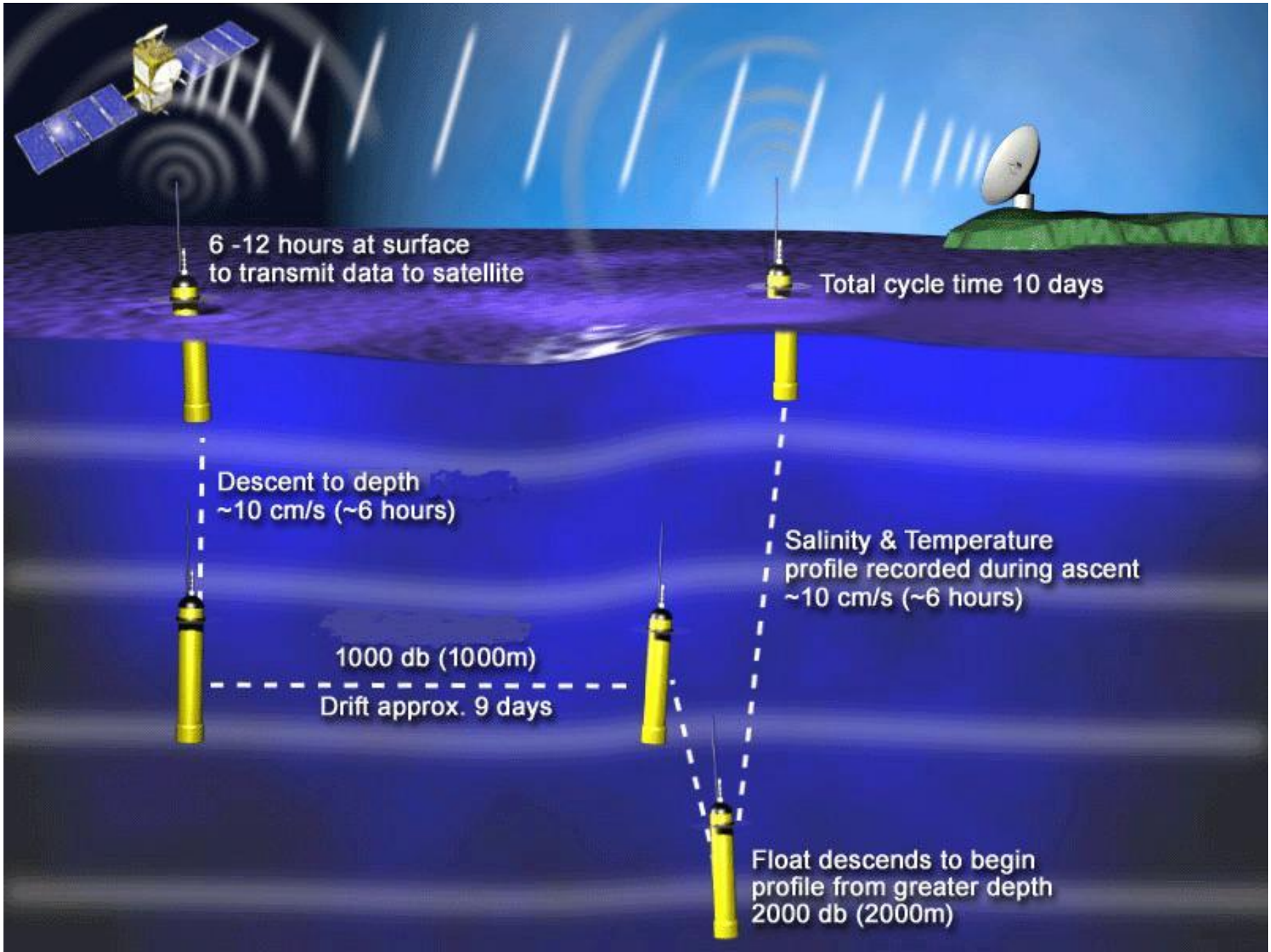
the matrices **B** and **R**

Observational Error Variance Matrix **R**

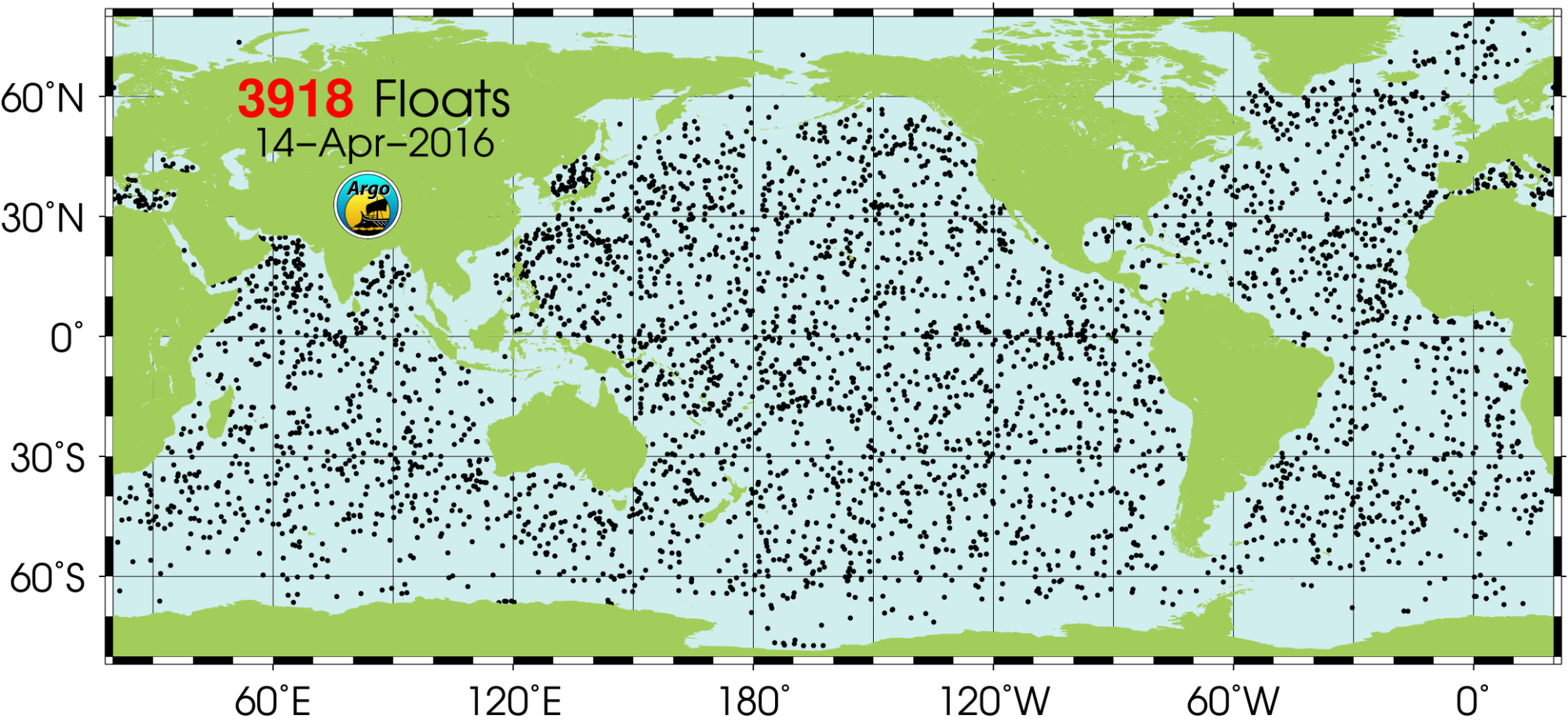
$$\mathbf{R} = E_o^2 \mathbf{I}, \qquad E_o^2 \equiv \left\langle \boldsymbol{\varepsilon}_o^T \boldsymbol{\varepsilon}_o \right\rangle$$

$\mathbf{I}$ → identity matrix

E_o^2 → Observational Error Variance


6 -12 hours at surface
to transmit data to satellite
Total cycle time 10 days
Descent to depth
~10 cm/s (~6 hours)
Salinity & Temperature
profile recorded during ascent
~10 cm/s (~6 hours)
1000 db (1000m)
Drift approx. 9 days
Float descends to begin
profile from greater depth
2000 db (2000m)

Argo – Part of the Integrated Global Observation Strategy



Effectively using the ocean topographic characteristics



A new spectral ocean data assimilation method without requiring *a priori* knowledge of matrix B

(2) OSD Method

Basis Functions

$$\nabla^2\phi_k = -\lambda_k\phi_{\mathrm{k},} \quad \left[b_1\mathbf{n}\bullet\nabla\phi_k + b_2\phi_k\right]|_\Gamma = 0, \quad k = 1,\ldots,\infty$$

ϕ_k → The eigen functions of the 2D Laplacian Operator

satisfaction of the same homogeneous boundary condition of the assimilated variable anomaly

$b_1 = 0$ → Dirichlet boundary condition

$b_2 = 0$ → Newmann boundary condition

$b_1 \neq 0, \; b_2 \neq 0 \;\rightarrow$ Cauchy boundary condition

Basis Function Matrix

Φ Matrix →

$$\mathbf{\Phi} = \{\phi_{kn}\} = \begin{bmatrix} \phi_1(\mathbf{r}_1) & \phi_2(\mathbf{r}_1) & \dots & \phi_K(\mathbf{r}_1) \\ \phi_1(\mathbf{r}_2) & \phi_2(\mathbf{r}_2) & \dots & \phi_K(\mathbf{r}_2) \\ \dots & \dots & \dots & \dots \\ \phi_1(\mathbf{r}_N) & \phi_2(\mathbf{r}_N) & \dots & \phi_K(\mathbf{r}_N) \end{bmatrix}$$

K → truncated mode number

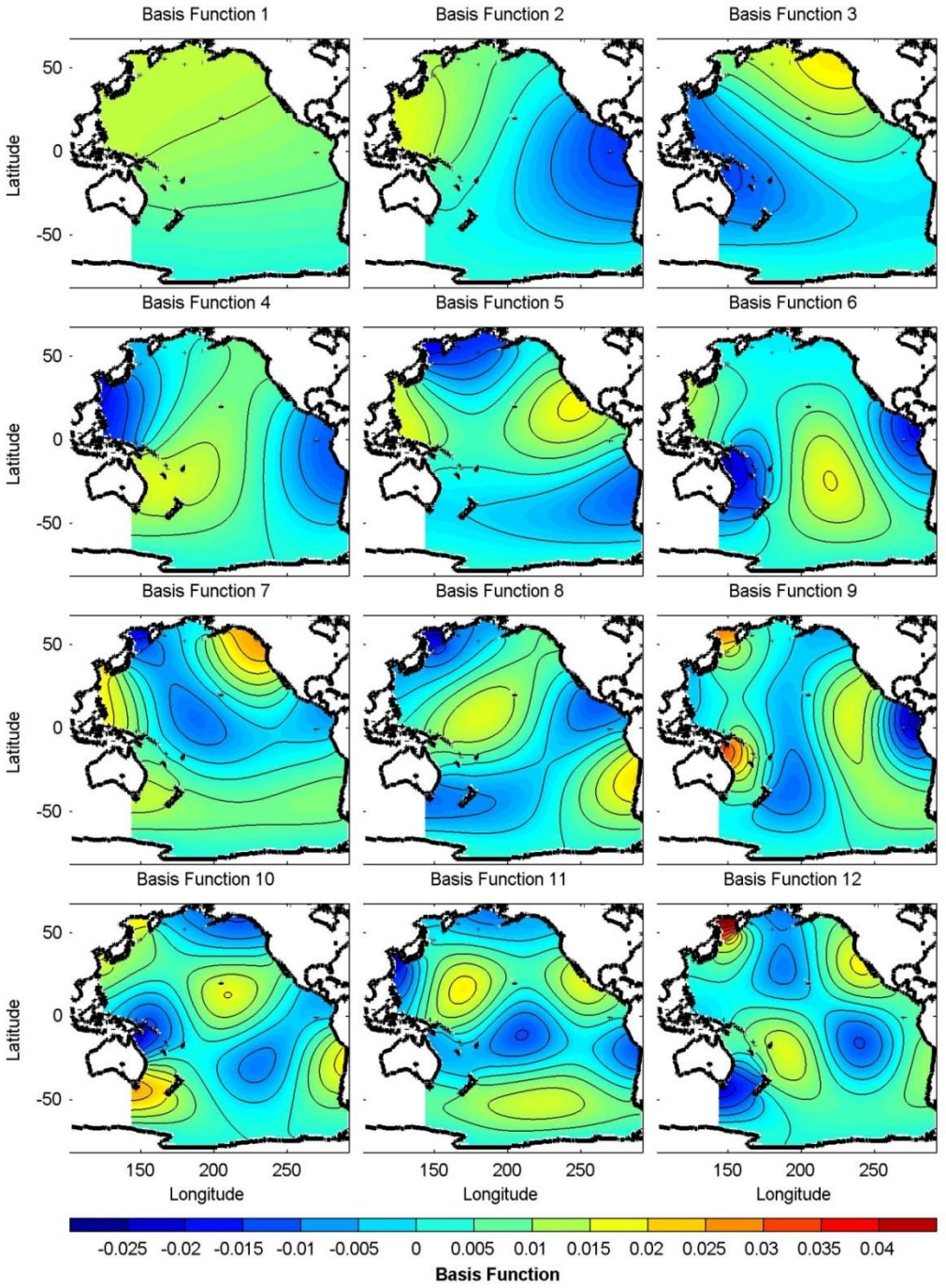
N → number of grid points

First 12 basis functions for the Pacific Ocean at the surface.

DBDB5

Dirichlet boundary condition at the southern boundary (Antarctic),

Newmann boundary condition elsewhere



Spectral Ocean Data Assimilation

$$\mathbf{c}_a = \mathbf{c}_b + f_n \mathbf{s}^{(K)}, \quad s_K(\mathbf{r}_n) \equiv \sum_{k=1}^{K} a_k \, \phi_k(\mathbf{r}_n),$$

$\mathbf{H} = [h_{mn}]$ → the $M \times N$ linear observation operator matrix

$$f_n \equiv \sum_{m=1}^{M} h_{nm}$$

$$\mathbf{F} = \begin{bmatrix} f_1 & 0 & 0 & 0 & 0 & 0 \\ 0 & f_2 & 0 & 0 & 0 & 0 \\ 0 & 0 & \ddots_i & 0 & 0 & 0 \\ 0 & 0 & 0 & f_n & 0 & 0 \\ 0 & 0 & 0 & 0 & \ddots & 0 \\ 0 & 0 & 0 & 0 & 0 & f_N \end{bmatrix}$$

$$\boldsymbol{\varepsilon}_a \equiv \mathbf{c}_a - \mathbf{c}_t = (\mathbf{c}_a - \mathbf{c}_b) + (\mathbf{c}_b - \mathbf{c}_t) = \boldsymbol{\varepsilon}_K + \boldsymbol{\varepsilon}_o$$

$$\boldsymbol{\varepsilon}_K \equiv \left[f_n \mathbf{s}^{(K)} - \mathbf{H}^T (\mathbf{c}_o - \mathbf{H}\mathbf{c}_b) \right], \quad \boldsymbol{\varepsilon}_o \equiv \mathbf{H}^T \mathbf{c}_o - \mathbf{c}_t \quad \left\langle \boldsymbol{\varepsilon}_o^T \boldsymbol{\varepsilon}_K \right\rangle = 0$$

$$E^2 = \left\langle \boldsymbol{\varepsilon}_a^T \boldsymbol{\varepsilon}_a \right\rangle = E_K^2 + E_o^2, \quad E_K^2 \equiv \left\langle \boldsymbol{\varepsilon}_K^T \boldsymbol{\varepsilon}_K \right\rangle, E_o^2 \equiv \left\langle \boldsymbol{\varepsilon}_o^T \boldsymbol{\varepsilon}_o \right\rangle$$

Steep-Descending Mode Truncation

$$\gamma_K = \ln\left[\frac{E_{K-1}^2 + 2E_{K-1}\sqrt{M/N}E_o + ME_o^2/N}{E_K^2 + 2E_K\sqrt{M/N}E_o + ME_o^2/N}\right], \qquad K = 2,3,...$$

E_o^2 → observational error variance

N → total number of grid points

M → total number of observational points

$$K_{OPT} = \max_{\gamma_K \geq \gamma_{th}}(K)$$

OSD Data Analysis/Assimilation

$$E^2 \to \min, \quad \partial E^2 / \partial a_k = \partial E^2_{K_{OPT}} / \partial a_k = 0, \quad k = 1, \ldots, K_{OPT}$$

$$E_K^2 = \sum_{n=1}^{N} \left(f_n \sum_{k=1}^{K_{OPT}} a_k \phi_{kn} - D_n \right)^2 \to \min$$

$$\sum_{k'=1}^{K} \sum_{n=1}^{N} \left(\phi_{kn} f_n \phi_{nk'} \right) a_{k'} = \sum_{n=1}^{N} \phi_{kn} f_n D_n, \qquad k = 1, 2, \ldots, K_{OPT}$$

$$\mathbf{\Phi F \Phi}^T \mathbf{A} = \mathbf{\Phi F D}, \qquad \mathbf{A} = \left[\mathbf{\Phi F \Phi}^T \right]^{-1} \mathbf{\Phi F D}$$

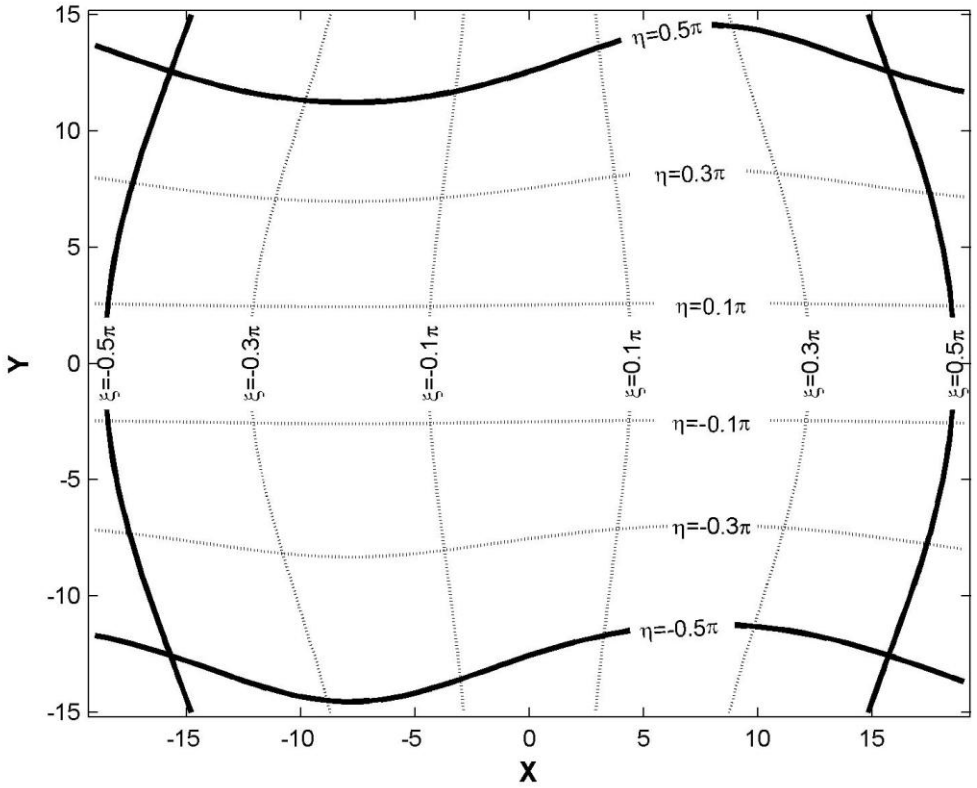
OSD → $$\mathbf{c}_a = \mathbf{c}_b + \mathbf{F \Phi}^T \left[\mathbf{\Phi F \Phi}^T \right]^{-1} \mathbf{\Phi H}^T \mathbf{d}$$

No Background Error Covariance Matrix Needed

Comparison between OSD/ OI

$$\frac{x}{10} - 0.3\cos\left(\frac{y}{8}\right)\sin\left(\frac{x}{10}\right) = \xi = \begin{cases} -\pi/2 & \text{(west)} \\ \pi/2 & \text{(east)} \end{cases}$$

$$\frac{y}{8} - 0.2\sin\left(\frac{x}{5}\right)\left[1 - \cos\left(\frac{y}{8}\right)\right] = \eta = \begin{cases} -\pi/2 & \text{(south)} \\ \pi/2 & \text{(north)} \end{cases}$$

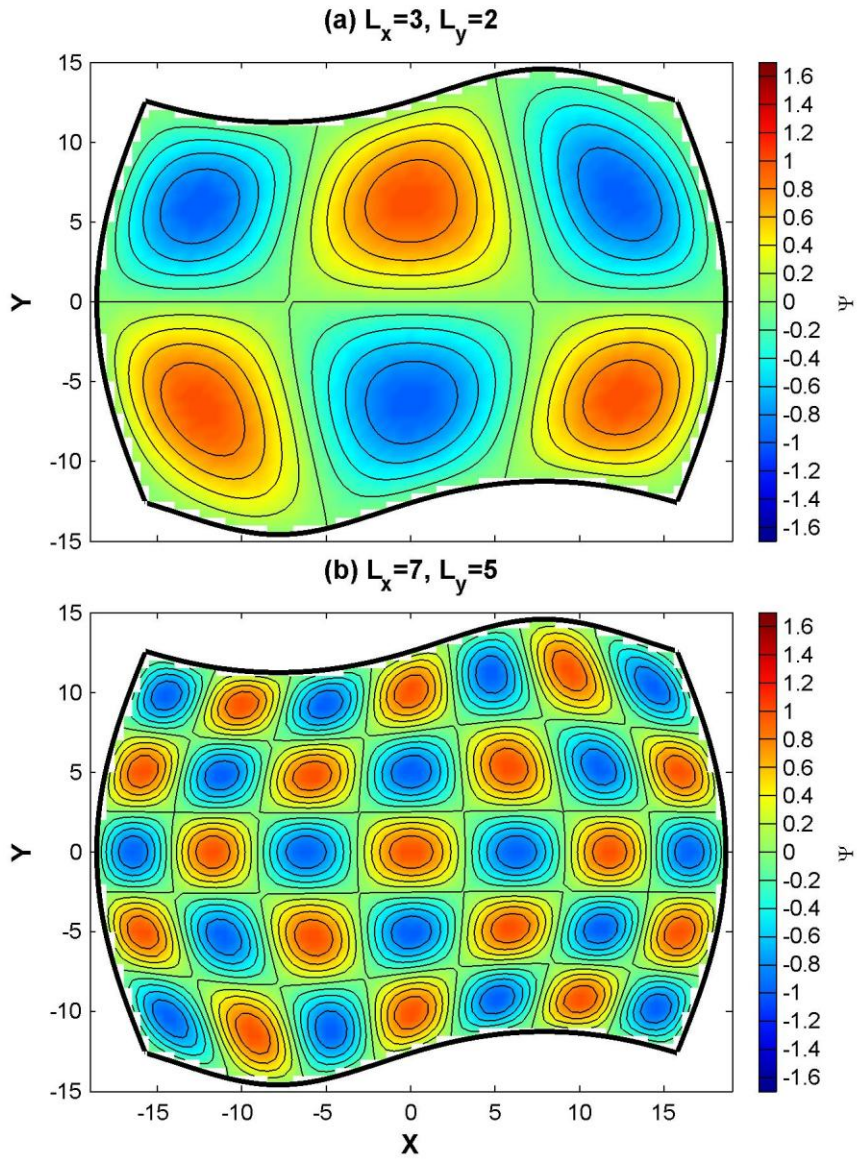


“Truth” – Analytical Streamfunction

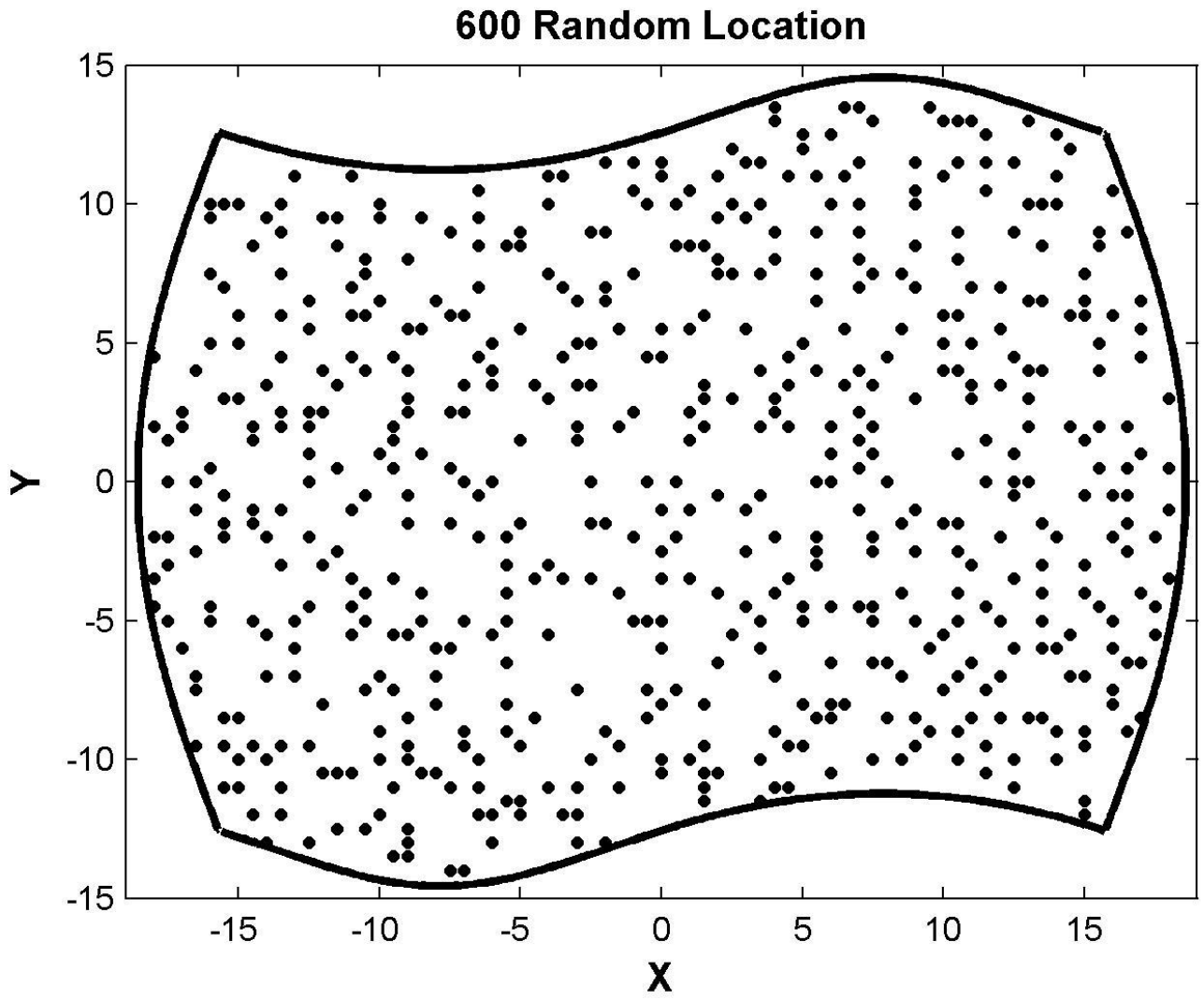
Large-Scale Eddies →

$$\begin{cases} \psi_t(x,y) = \cos\left[L_x\xi(x,y)\right]\cos\left[L_y\eta(x,y)+\beta\right] \\ \xi = \dfrac{x}{10} - 0.3\cos\left(\dfrac{y}{8}\right)\sin\left(\dfrac{x}{10}\right), \\ \eta = \dfrac{y}{8} - 0.2\sin\left(\dfrac{x}{5}\right)\left[1-\cos\left(\dfrac{y}{8}\right)\right] \end{cases}$$

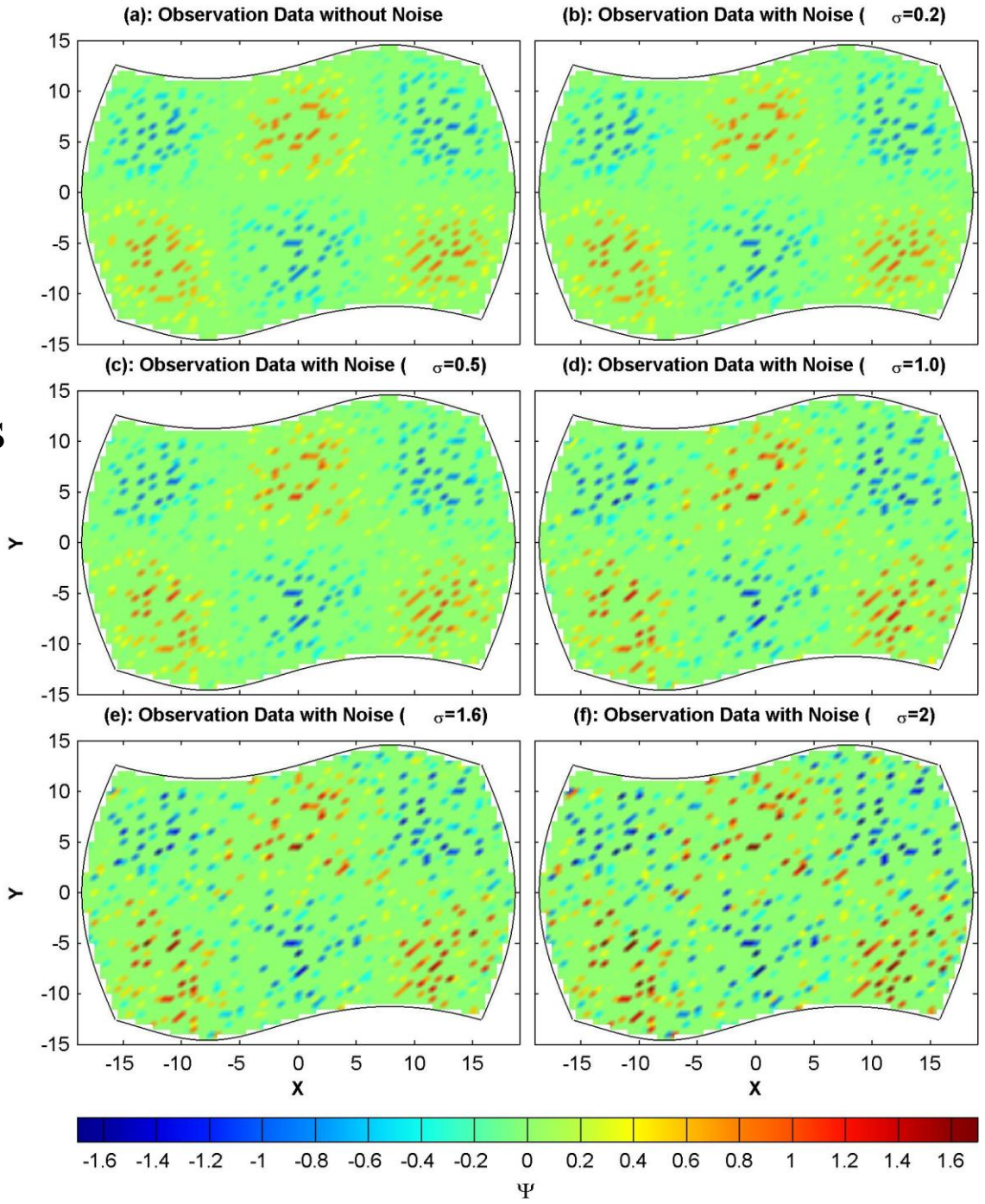
Small-Scale Eddies →



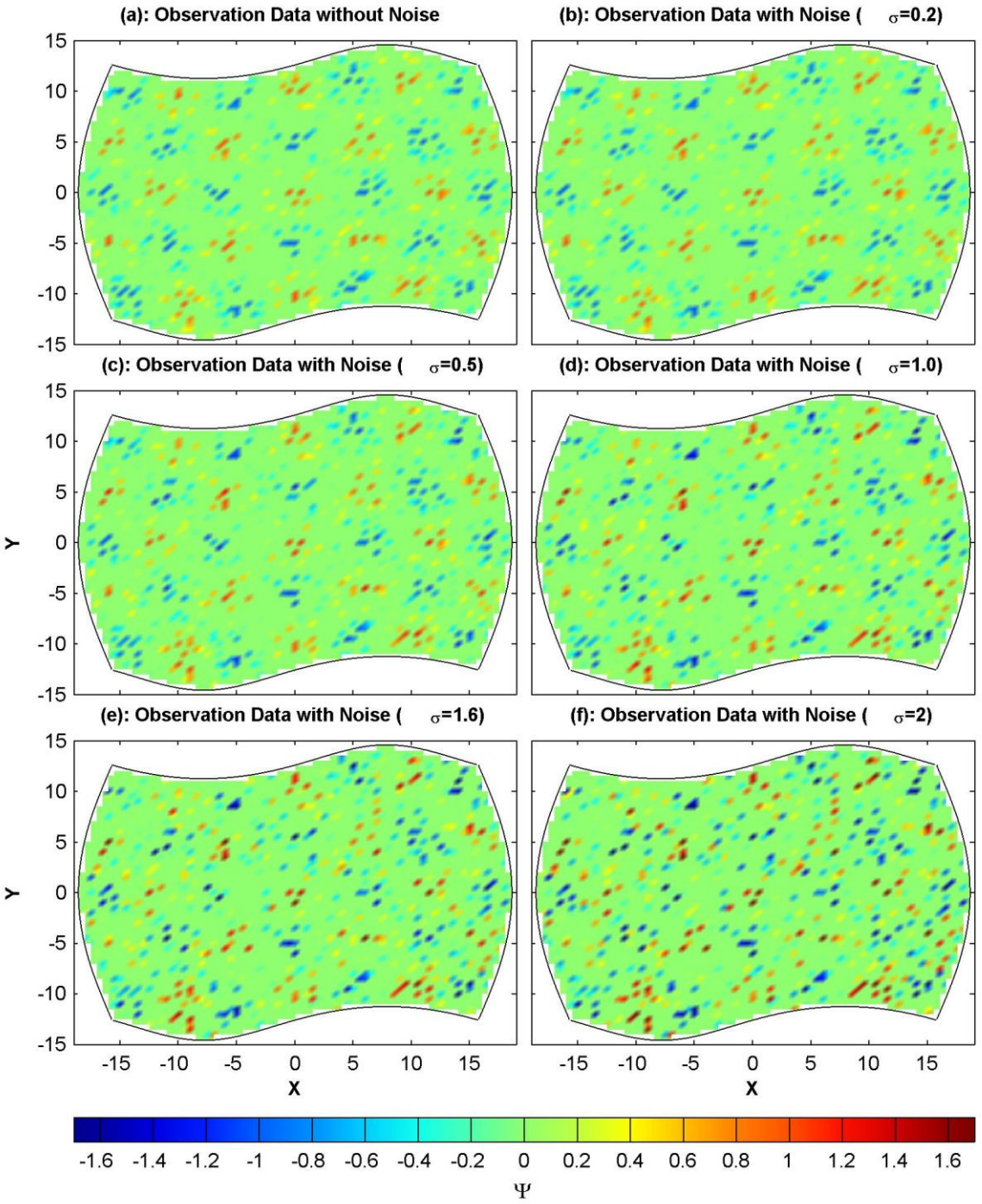
Randomly selected locations (total: 600) inside domain as “observational” points



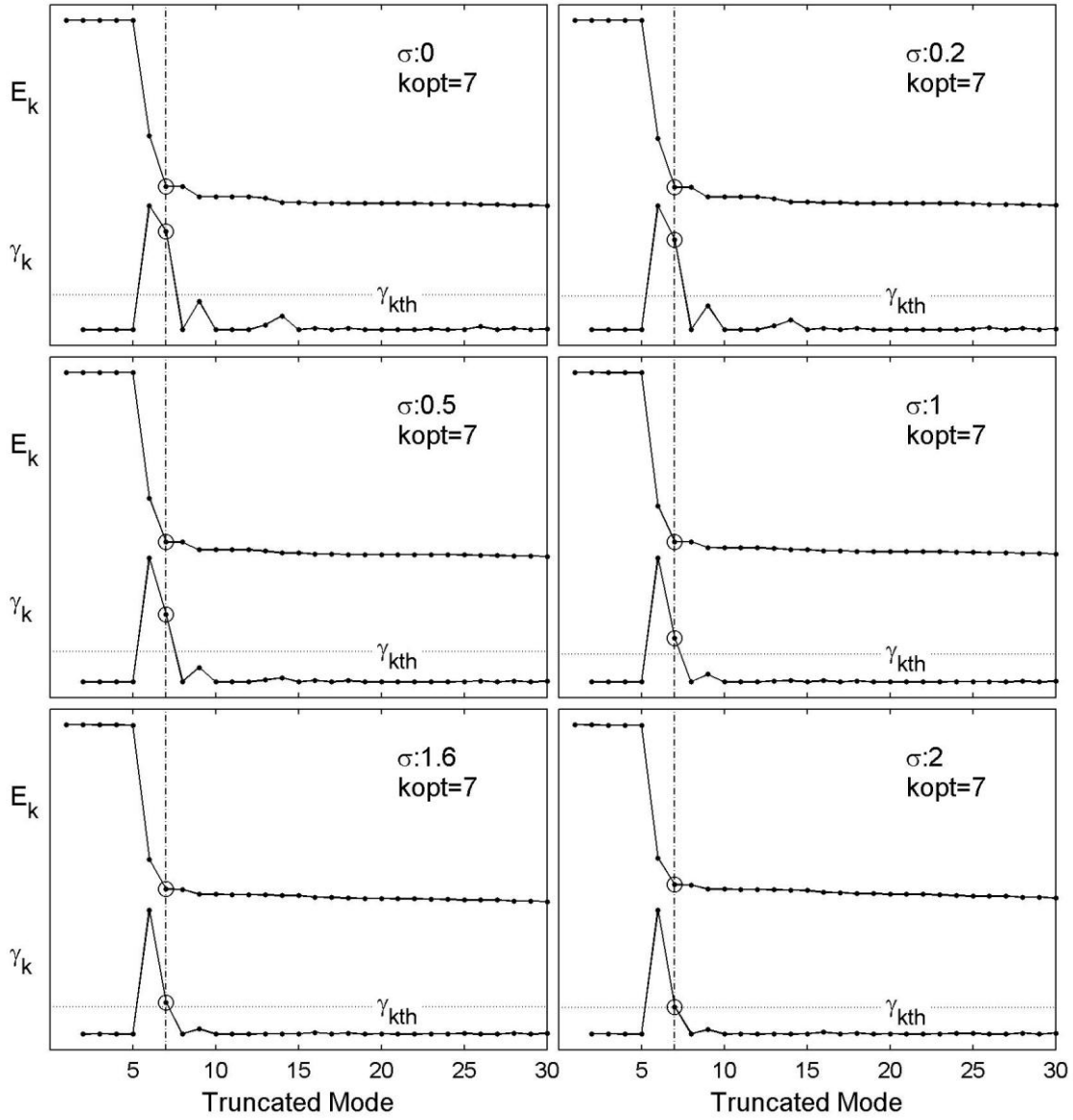
"Observational" data (ψ_o) from "truth" (large-scale) plus white Gaussian noises of zero mean and various standard deviations: (a) 0 (i.e., no noise) (b) 0.2, (c) 0.5, (d) 1.0, (e) 1.6, and (f) 2.0.



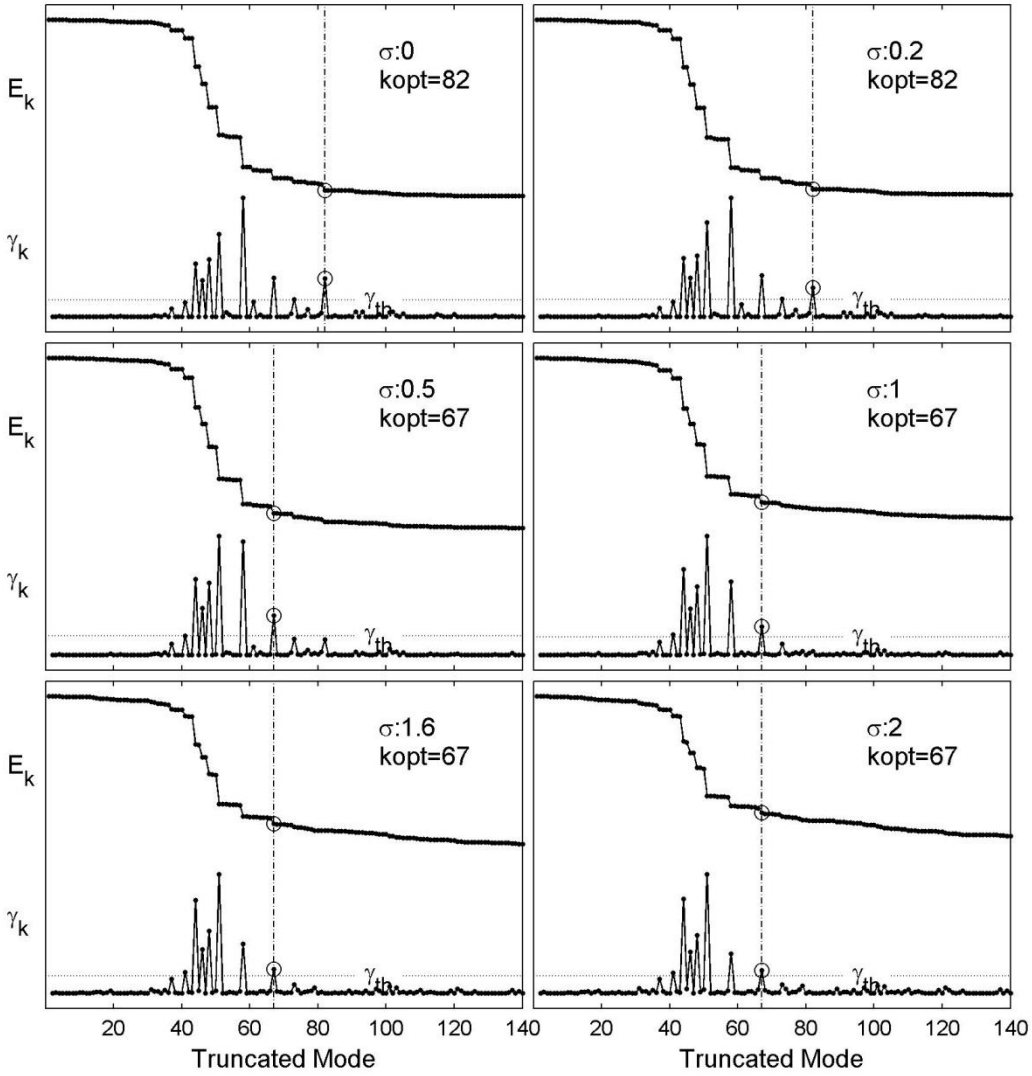
"Observational" data (ψ_o) from "truth" (small-scale) plus white Gaussian noises of zero mean and various standard deviations: (a) 0 (i.e., no noise) (b) 0.2, (c) 0.5, (d) 1.0, (e) 1.6, and (f) 2.0.



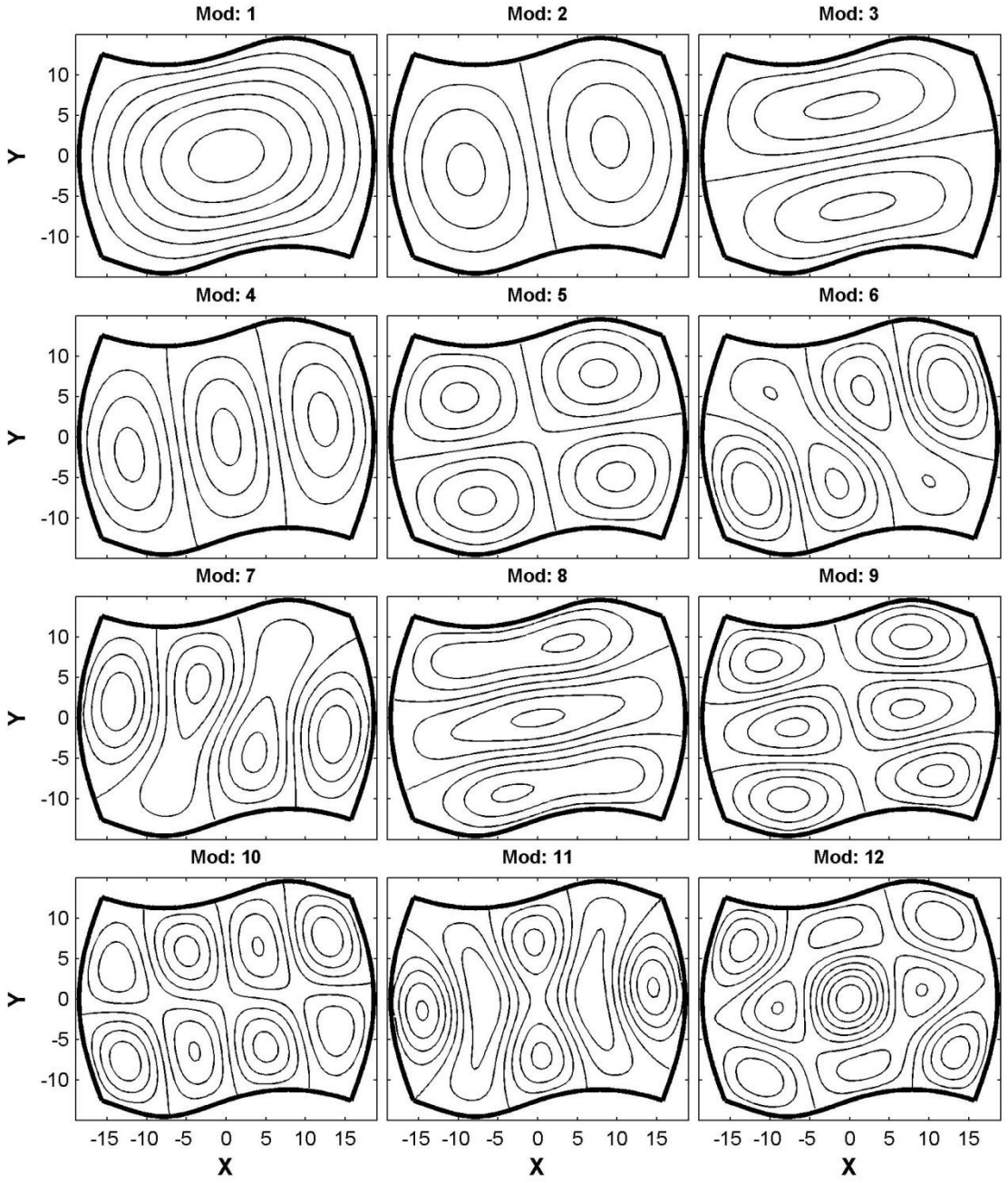
Mode truncation for large-scale “observational data”



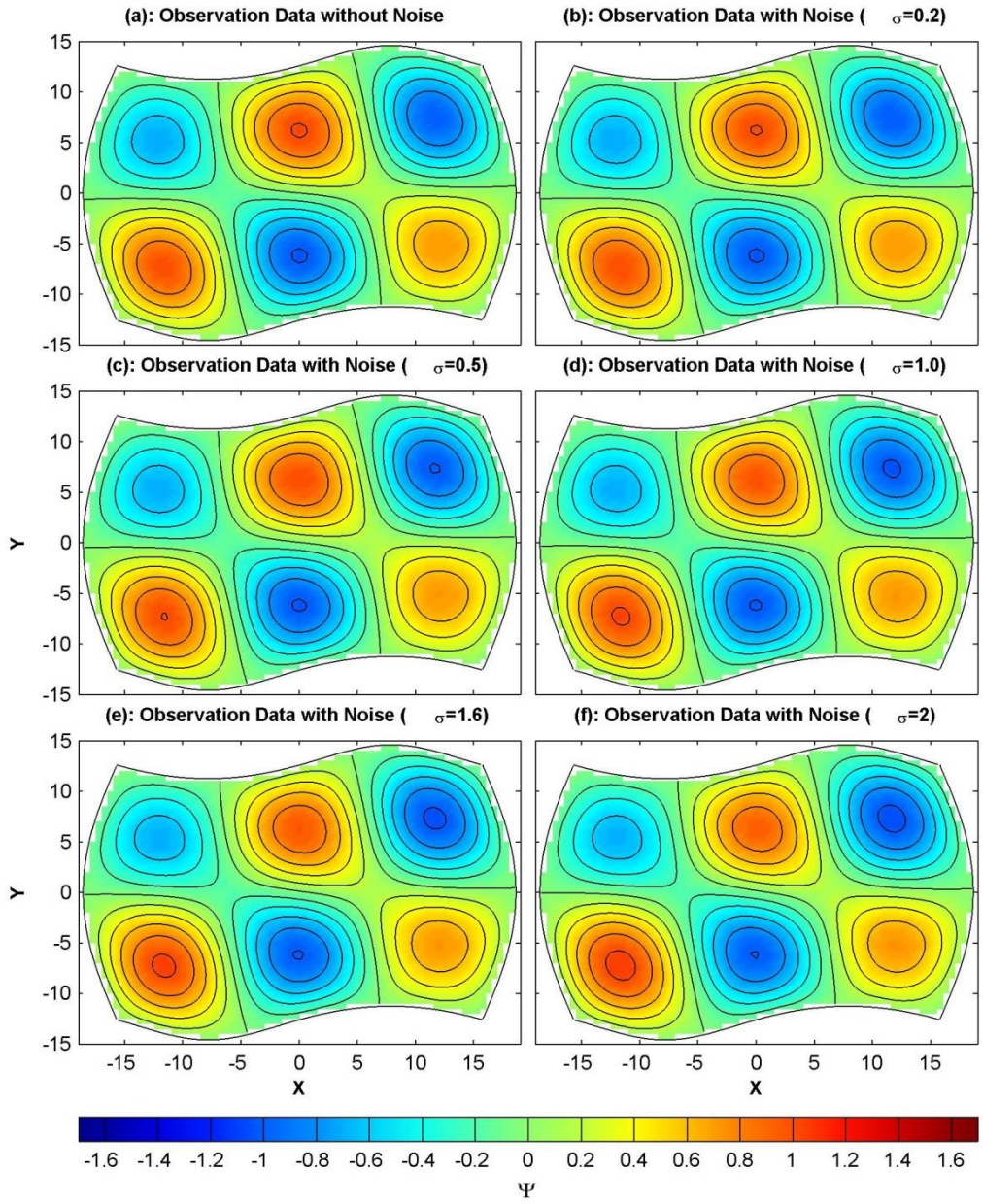
Mode truncation for small-scale "observational data"



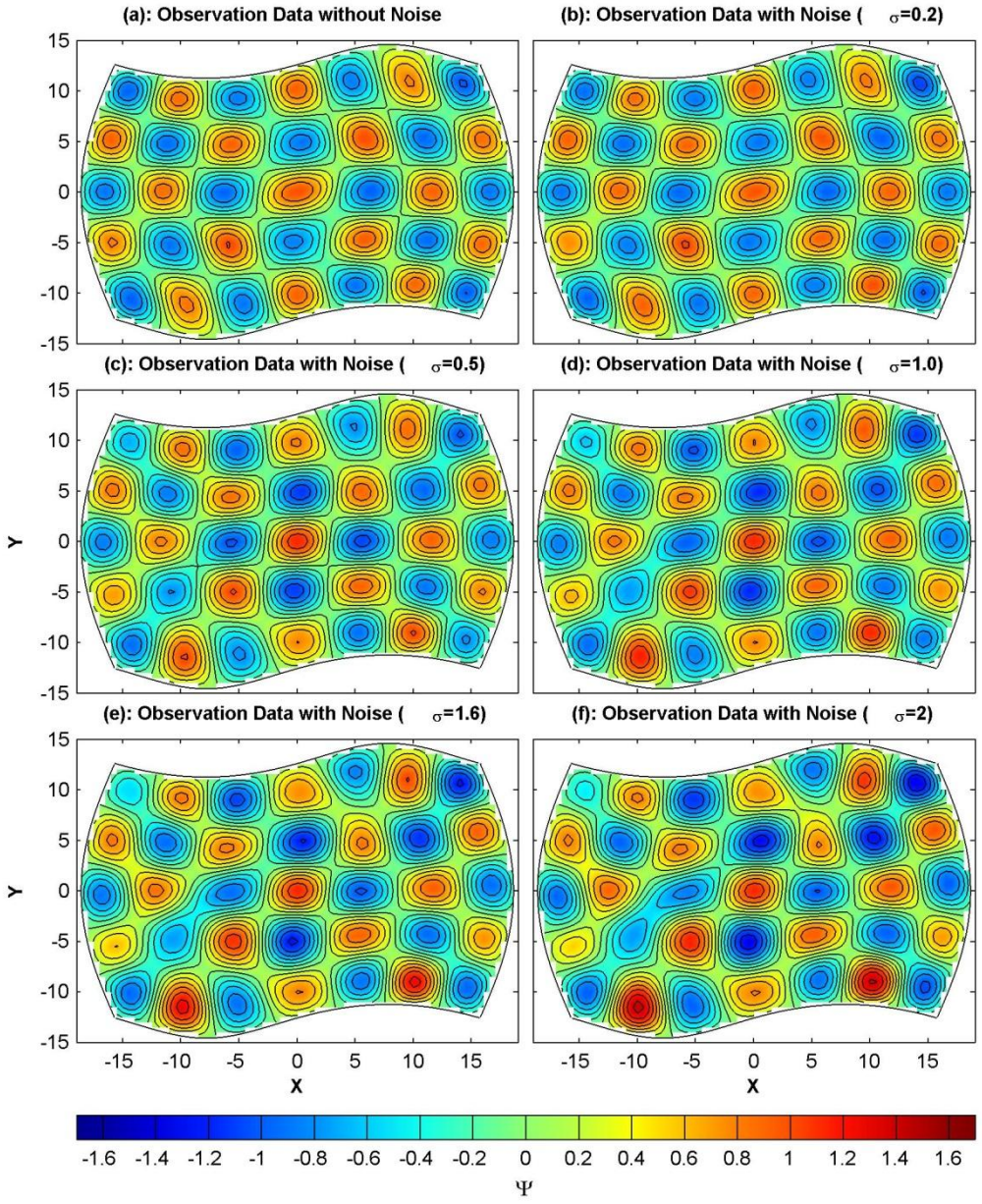
First 12 Basis Functions



Analysis field ψ_a obtained by the OSD Method



Analysis field ψ_a obtained by the OSD



Gaussian Covariance Function for **B**-Matrix (Bretherton et al. 1976)

Assumption → statistically stationary and homogeneous

$\mathbf{B} = \left[b_{ij} \right]_{N \times N}$ → between two grid points $\mathbf{r}_i$ and $\mathbf{r}_j$

$$b_{ij} = \left(1 - \frac{r_{ij}^2}{r_b^2} \right) \exp\left(-\frac{r_{ij}^2}{r_a^2} \right), \quad r_{ij}^2 = \left| \mathbf{r}_i - \mathbf{r}_j \right|^2$$

Two user-input parameters → r_a, r_b

Observational Error Variance Matrix **R**

$$\mathbf{R} = E_o^2 \mathbf{I}, \qquad E_o^2 \equiv \left\langle \boldsymbol{\varepsilon}_o^T \boldsymbol{\varepsilon}_o \right\rangle$$

$\mathbf{I}$ → identity matrix

E_o^2 → Observational Error Variance

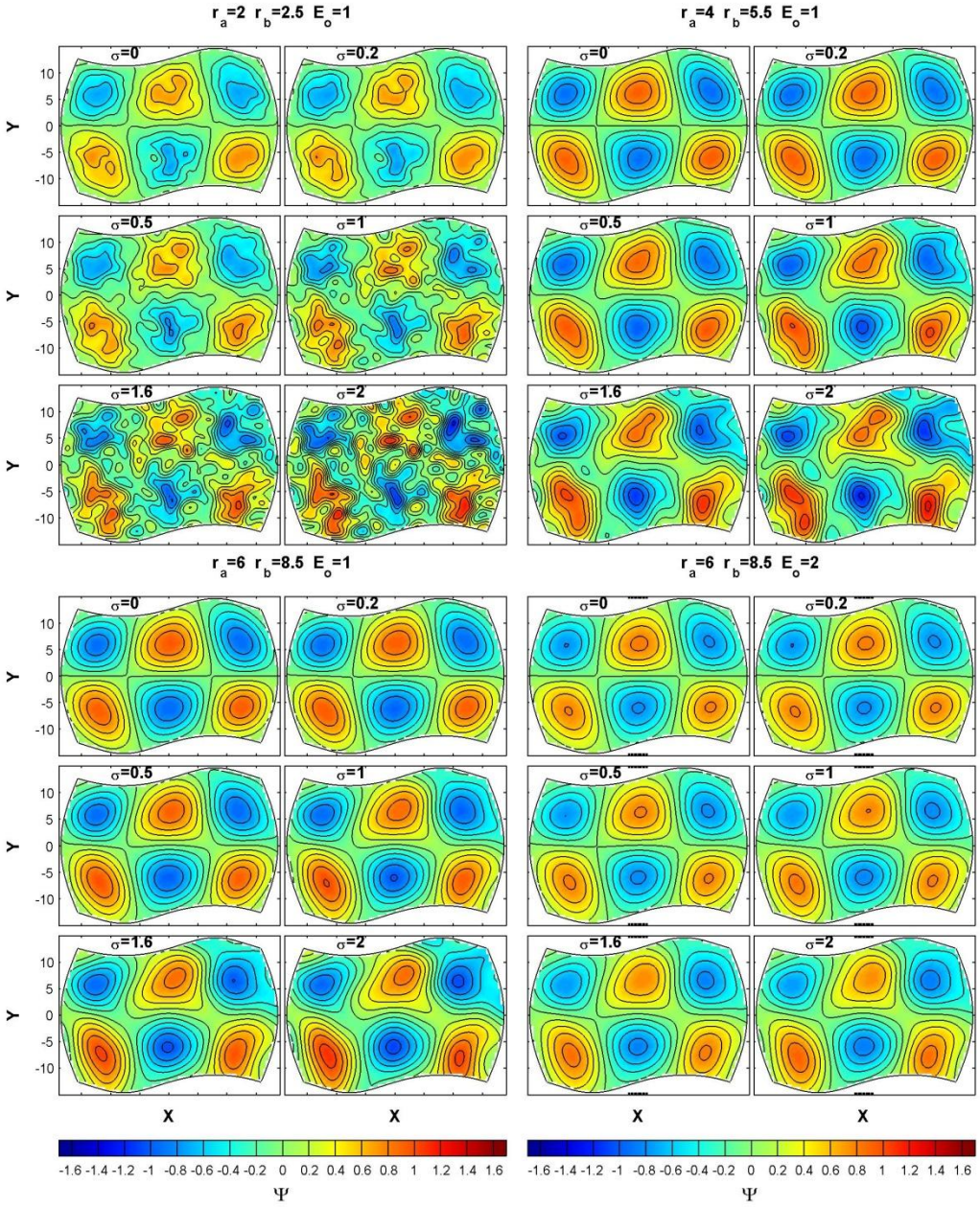
Analysis field ψ_a obtained by the OI – large eddies

$r_a = 2$
$r_b = 2.5$
$E_o = 1$

$r_a = 4$
$r_b = 5.5$
$E_o = 1$

$r_a = 6$
$r_b = 8.5$
$E_o = 1$

$r_a = 6$
$r_b = 8.5$
$E_o = 2$



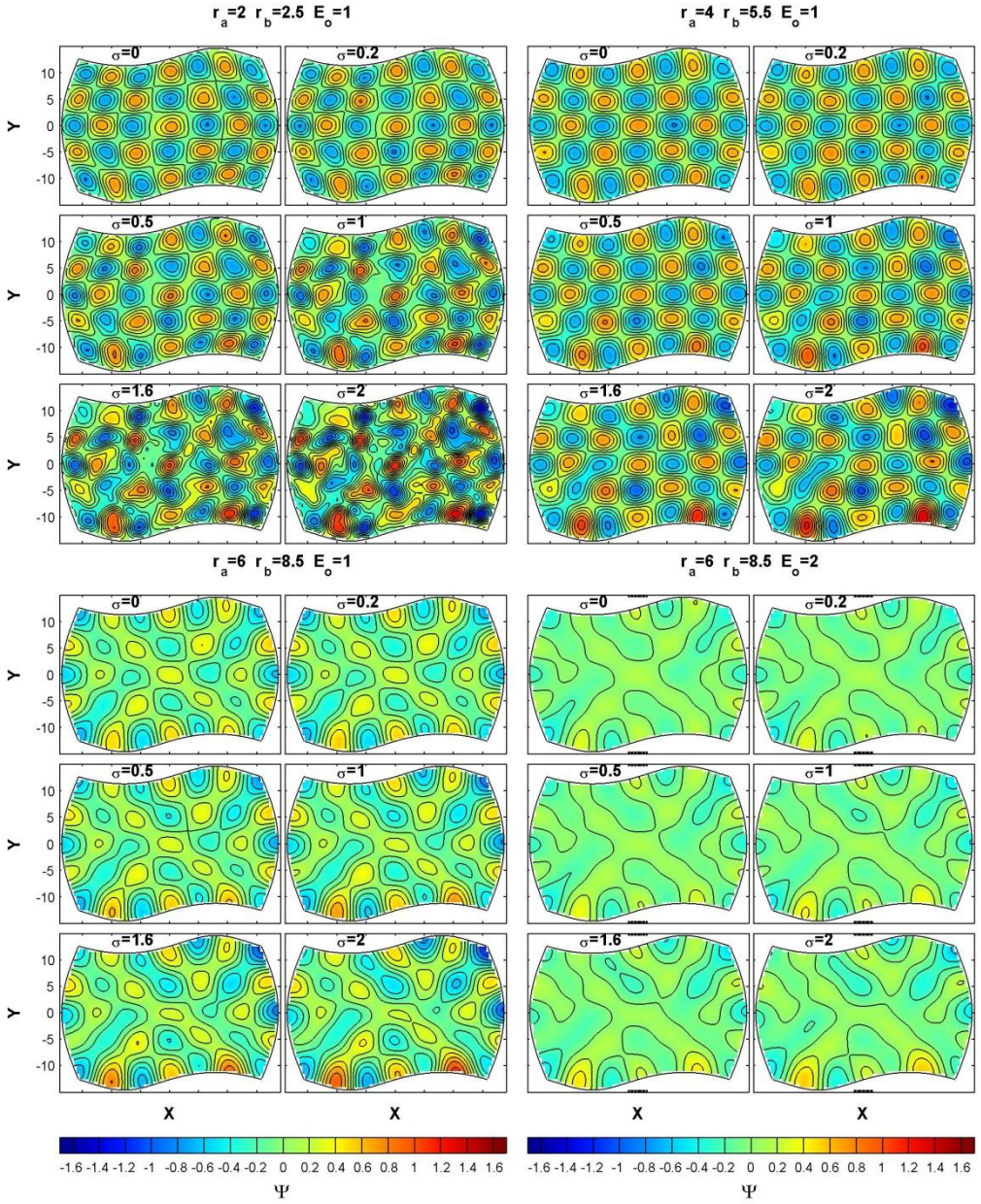
Analysis field ψ_a obtained by the OI – small eddies

$r_a = 2$
$r_b = 2.5$
$E_o = 1$

$r_a = 4$
$r_b = 5.5$
$E_o = 1$

$r_a = 6$
$r_b = 8.5$
$E_o = 1$

$r_a = 6$
$r_b = 8.5$
$E_o = 2$



Error Comparison Between OI and OSD

$$R^{OSD}(\sigma) = \sqrt{\frac{1}{N}\sum_{n=1}^{N}\left[\psi_a^{OSD}(\mathbf{r}_n,\sigma) - \psi_t(\mathbf{r}_n)\right]^2}$$

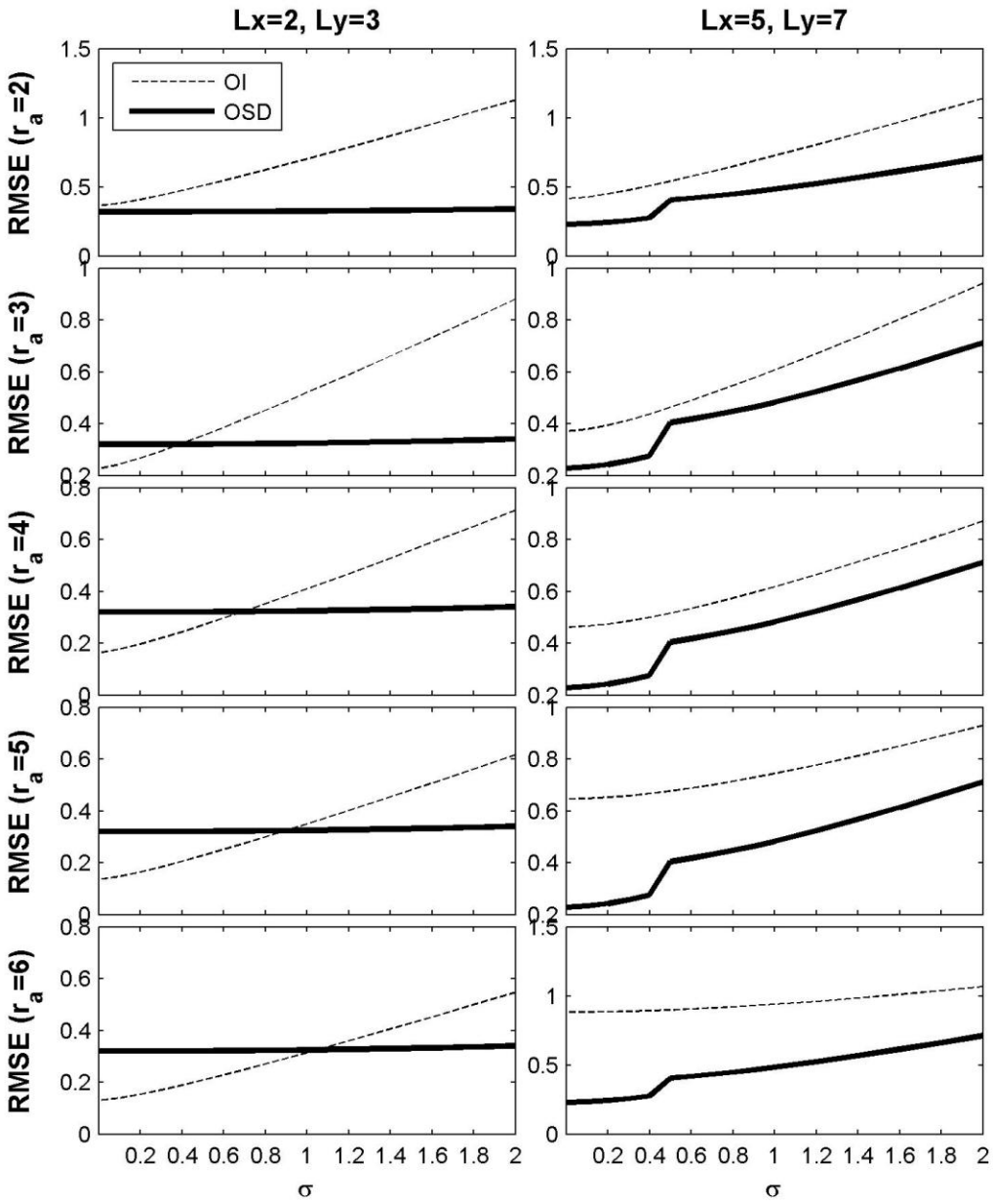
$$R^{OI}(\sigma, r_a) = \sqrt{\frac{1}{NP_bP_E}\sum_{r_b}\sum_{E_o}\sum_{n=1}^{N}\left[\psi_a^{OI}(\mathbf{r}_n,\sigma,r_a,r_b,E_o) - \psi_t(\mathbf{r}_n)\right]^2}$$

$$R^{OI}(\sigma, r_b) = \sqrt{\frac{1}{NP_aP_E}\sum_{r_a}\sum_{E_o}\sum_{n=1}^{N}\left[\psi_a^{OI}(\mathbf{r}_n,\sigma,r_a,r_b,E_o) - \psi_t(\mathbf{r}_n)\right]^2}$$

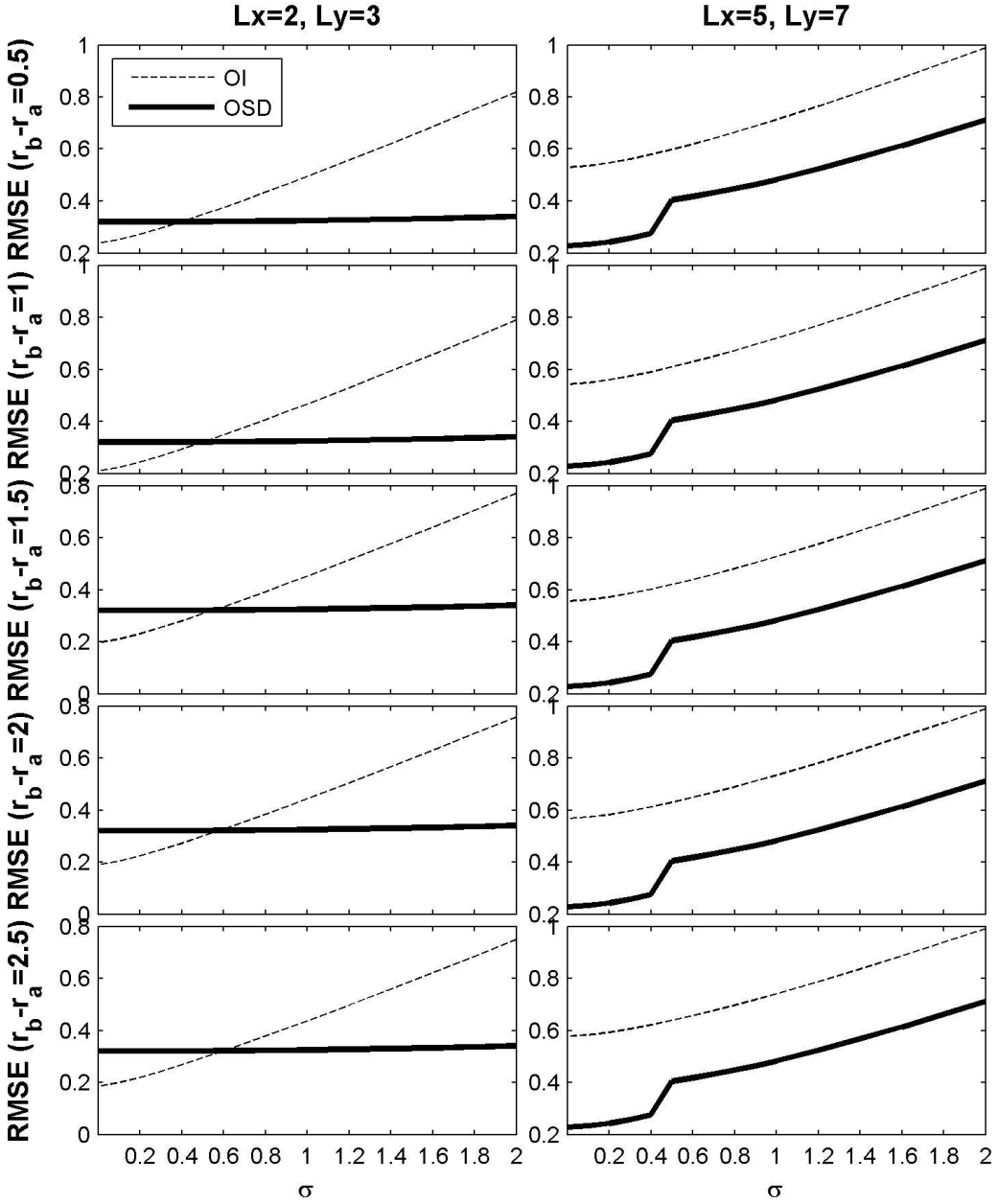
$$R^{OI}(\sigma, E_o) = \sqrt{\frac{1}{NP_aP_b}\sum_{r_b}\sum_{r_b}\sum_{n=1}^{N}\left[\psi_a^{OI}(\mathbf{r}_n,\sigma,r_a,r_b,E_o) - \psi_t(\mathbf{r}_n)\right]^2}$$

$(P_a, P_b, P_E) \rightarrow$ total numbers of (r_a, r_b, E_o)

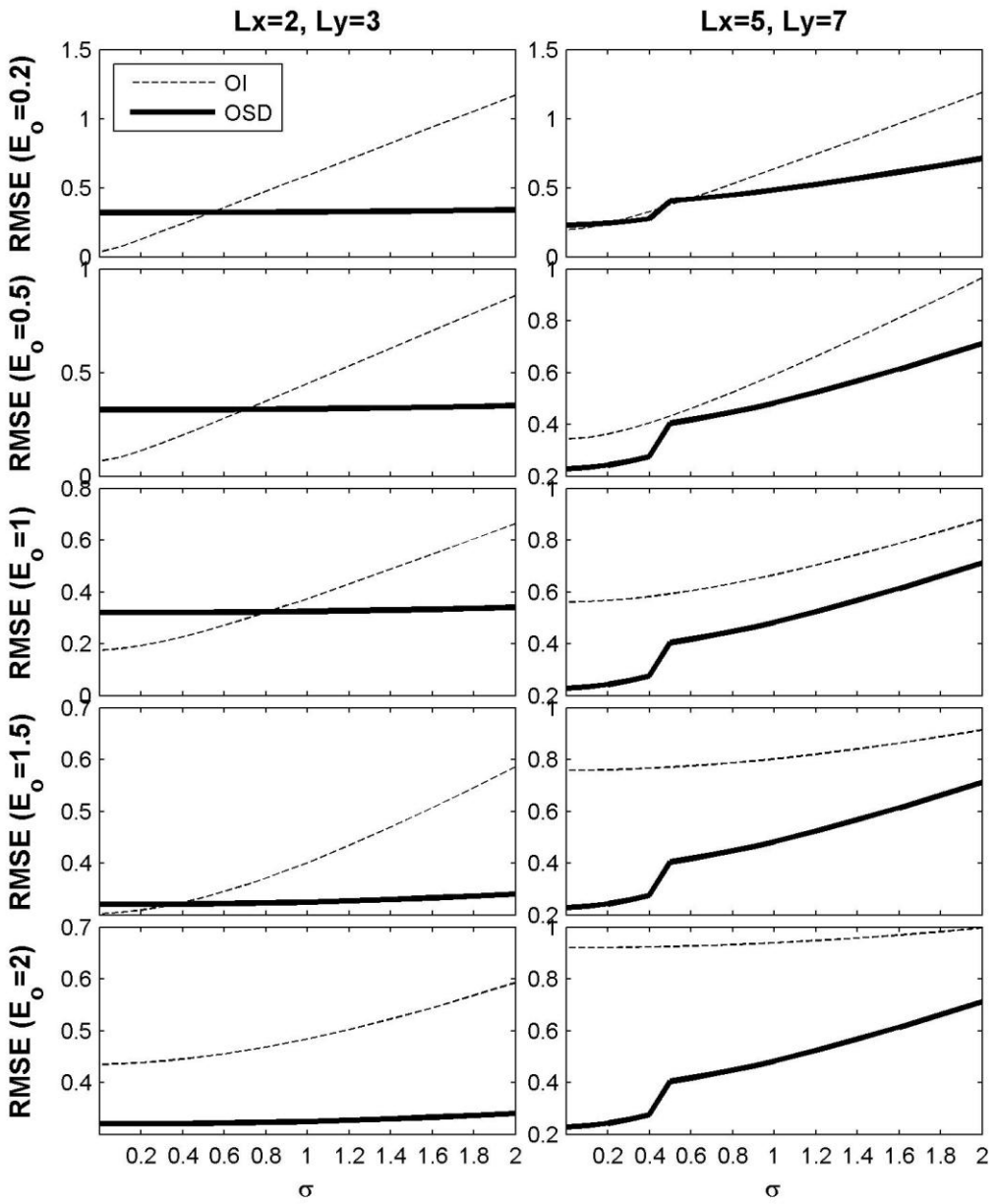
Comparison between $R^{OI}(\sigma, r_a)$ and $R^{OSD}(\sigma)$



Comparison between $R^{OI}(\sigma, r_b - r_a)$ and $R^{OSD}(\sigma)$

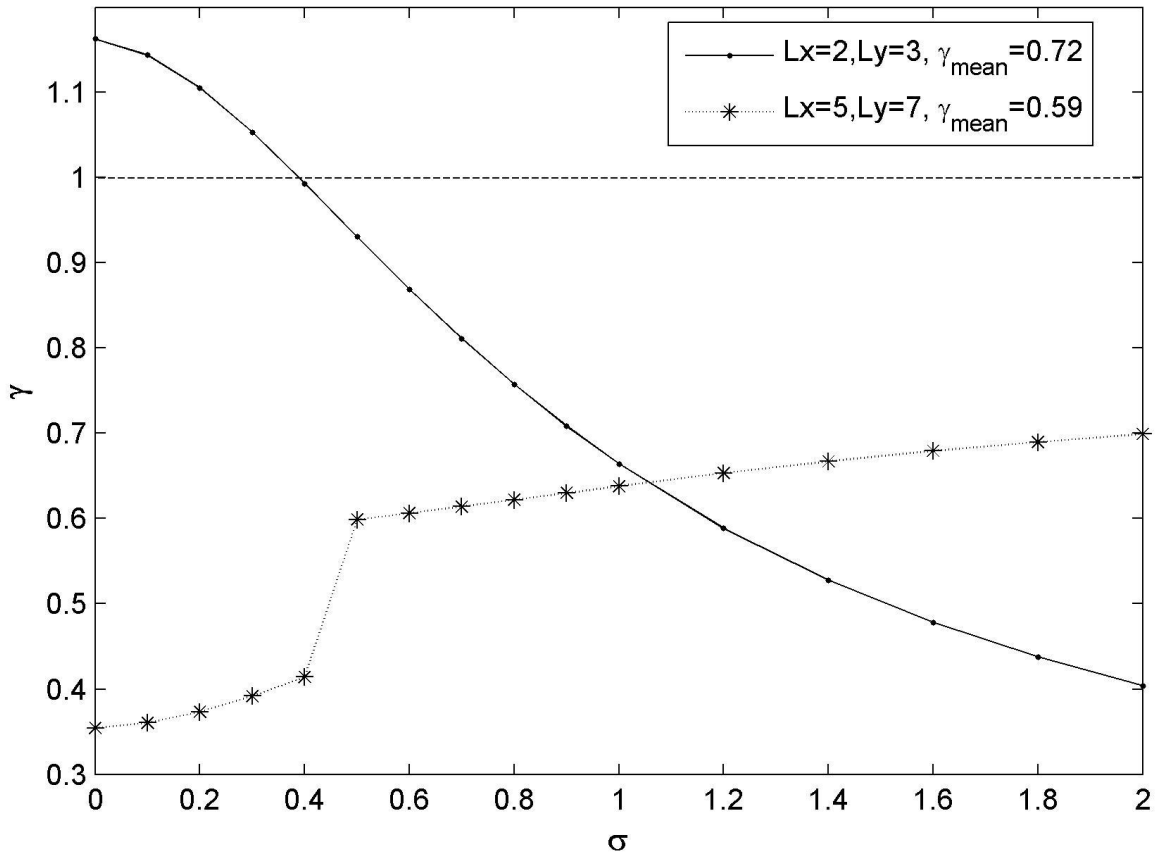


Comparison between $R^{OI}(\sigma, E_o)$ and $R^{OSD}(\sigma)$



$$\gamma(\sigma) = \frac{R^{OSD}(\sigma)}{\hat{R}^{OI}(\sigma)}$$

$$\hat{R}^{OI}(\sigma) \equiv \sqrt{\frac{1}{NP_aP_bP_E}\sum_{r_a}\sum_{r_b}\sum_{E_o}\sum_{n=1}^{N}\left[\psi_a^{OI}(\mathbf{r}_n,\sigma,r_a,r_b,E_o)-\psi_t(\mathbf{r}_n)\right]^2}$$



$$\hat{\gamma} = \frac{1}{2}\int_0^2 \gamma(\sigma)d\sigma = \begin{cases} 0.72 & \text{for large-scale eddy field} \\ 0.59 & \text{for small-scale eddy field} \end{cases}$$

(1) The overall error for the OSD is 72% (59%) of the OI for the large-scale (small-scale) eddy field.

(1) No any user-input parameter is needed.

(3) Synoptic Monthly Gridded World Ocean Database

Synoptic monthly gridded 3D World Ocean Database temperature and salinity from January 1945 to December 2014 (NCEI Accession 0140938)

Synoptic Monthly Gridded WOD Absolute Geostrophic Velocity (SMG-WOD-V) (January 1945 - December 2014) with the P-Vector Method (NCEI Accession 0146195)

Synoptic monthly gridded GTSPP from January 1990 to December 2009 (NCEI Accession 0138647)

Monthly Gridded Temperature at 10 m in the Atlantic Ocean



Monthly Gridded Temperature at 200 m in the Atlantic Ocean



Monthly Gridded Temperature at 1000 m in the Atlantic Ocean



Monthly Gridded Temperature at 10 m in the Pacific Ocean



Monthly Gridded Temperature at 200 m in the Pacific Ocean



Monthly Gridded Temperature at 1000 m in the Pacific Ocean



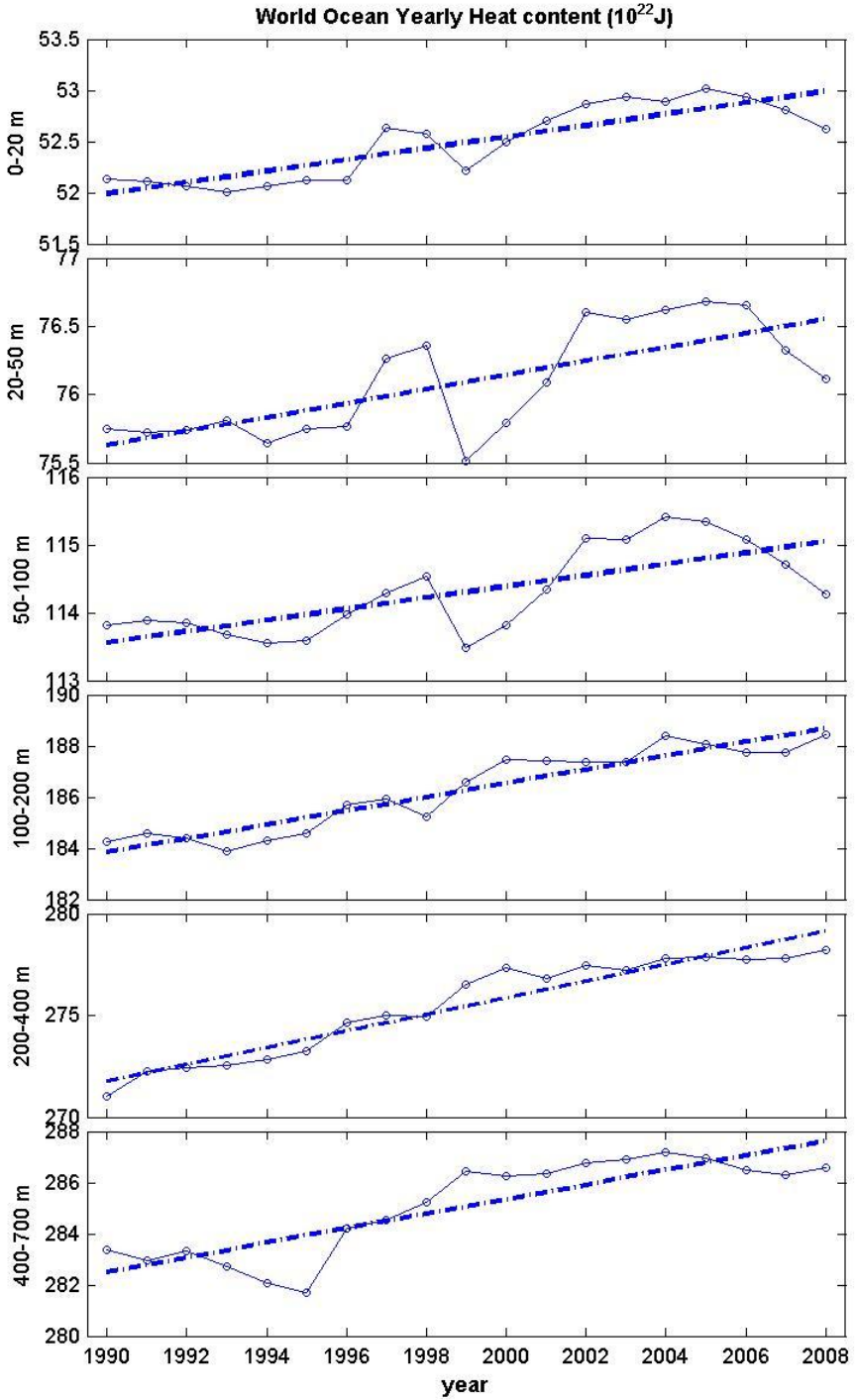
Upper Ocean (0-300 m) Heat Content

$$HC = \int_{-h}^{0} \rho c T dz$$

$HC = HC_{\text{mean}} + HC_{\text{seasonal}} + HC_{\text{anomaly}}$

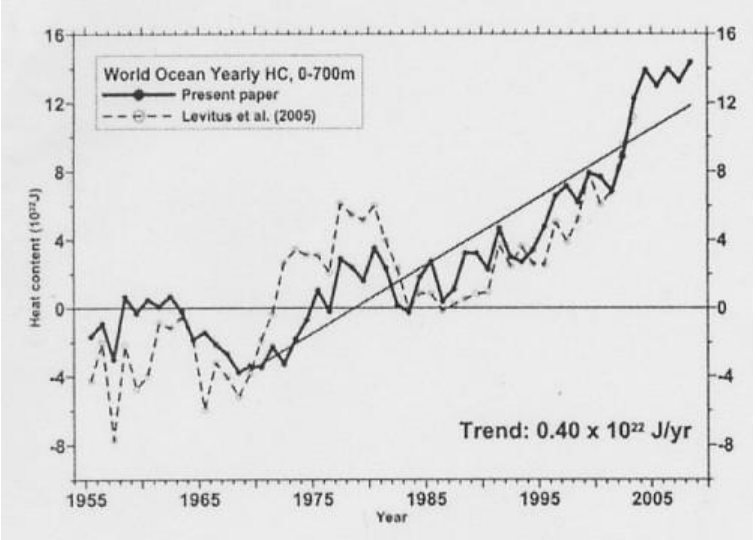
EOF Analysis → HC_{anomaly}

→ Global Ocean Dipole Modes


World Ocean Yearly Heat content (10^{22}J)
0-20 m
20-50 m
50-100 m
100-200 m
200-400 m
400-700 m
53.5
53
52.5
52
51.5
77
76.5
76
75.5
116
115
114
113
190
188
186
184
182
280
275
270
288
286
284
282
280
1990
1992
1994
1996
1998
2000
2002
2004
2006
2008
year

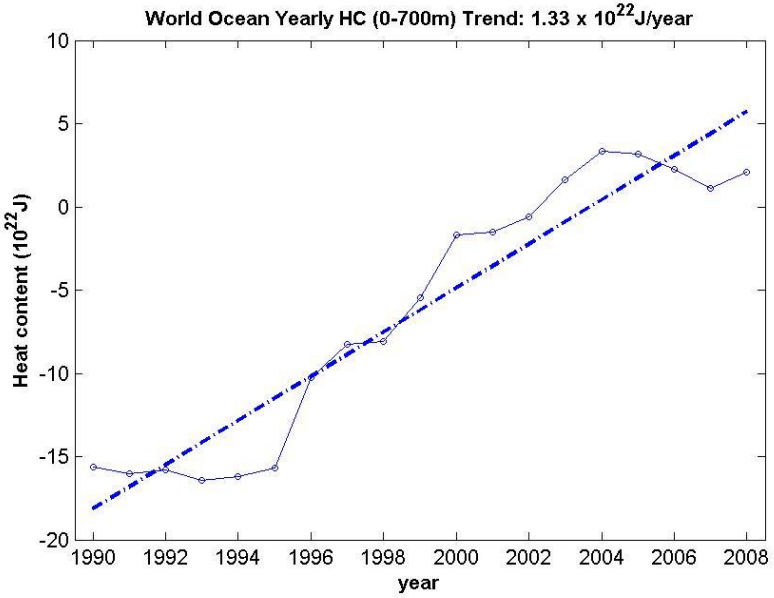
Trend of Upper Ocean (0-700 m) Heat Content

0.4 X 10^{22} J/yr
(1958-2008)
(Levitus et al.,GRL, 2009)
Without Argo data

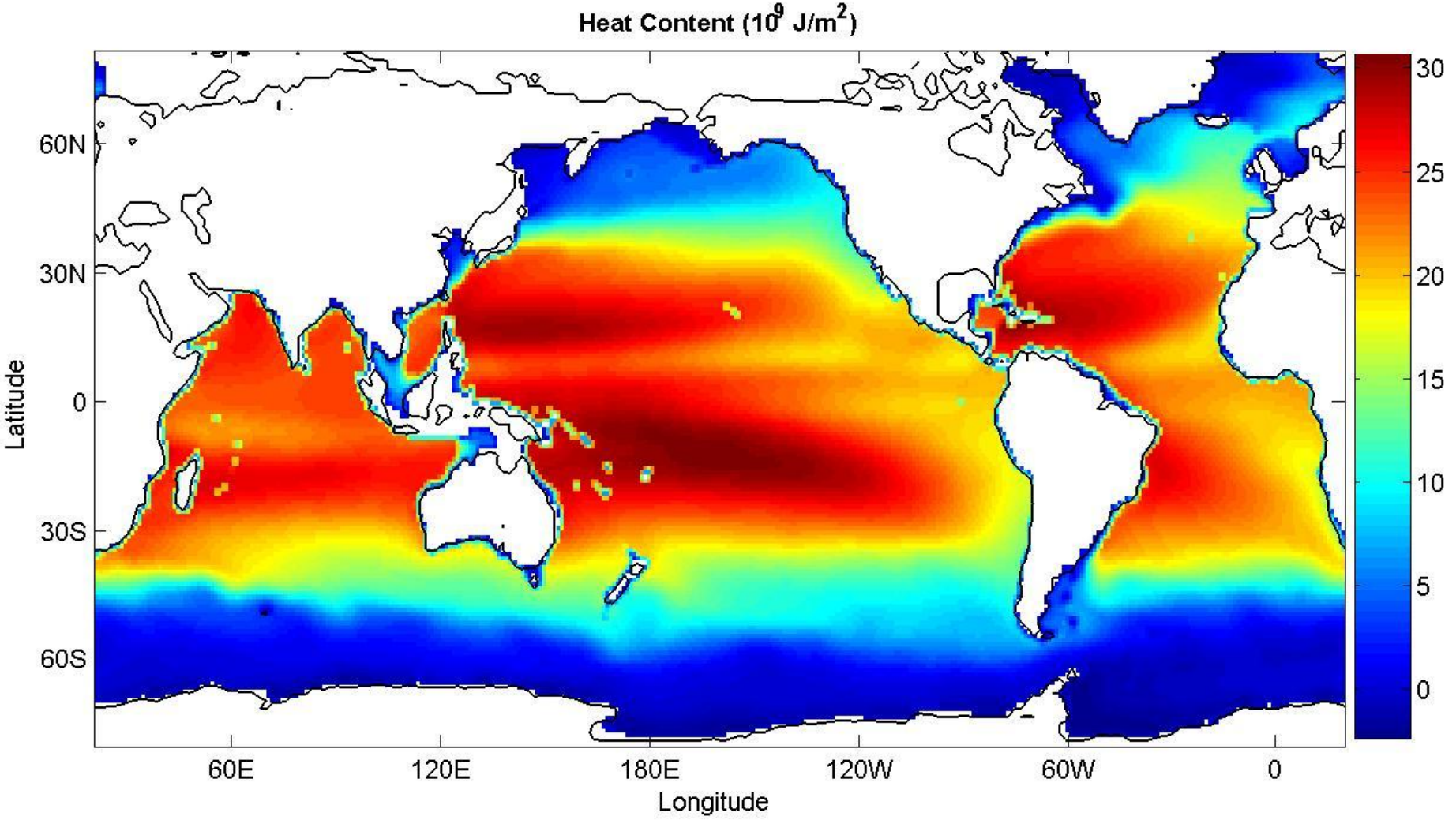


1.3 X 10^{22} J/yr
(1990-2008)

With Argo data

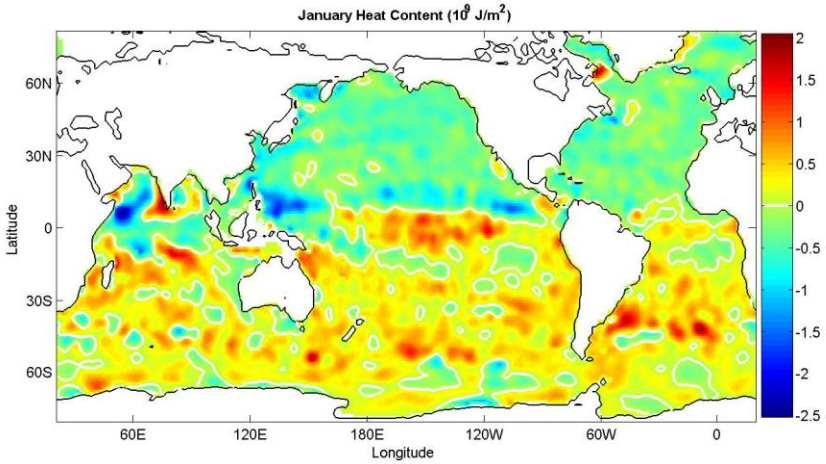


Upper Ocean (0-300 m) Mean Heat Content (J/m^2) (1990-2009)

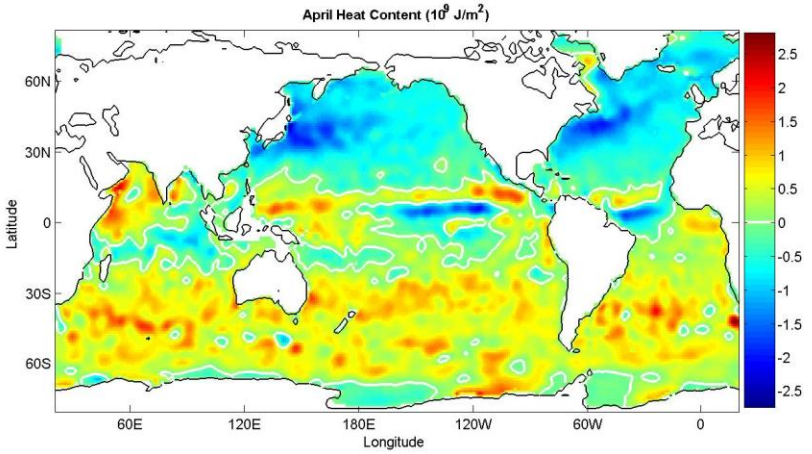


Seasonal Variability of Upper Ocean (0-300 m) Heat Content (J/m^2) (1990-2009)

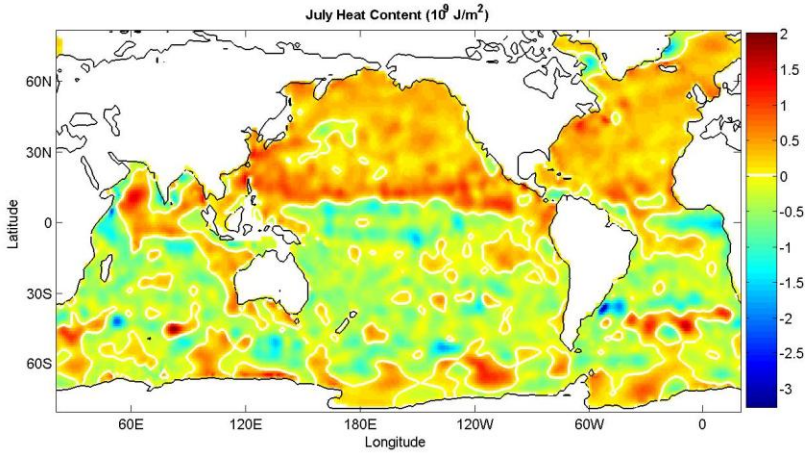
January



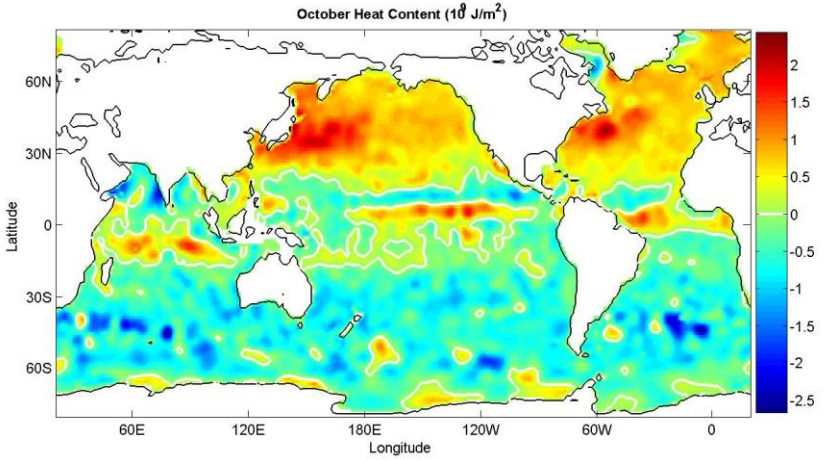
April



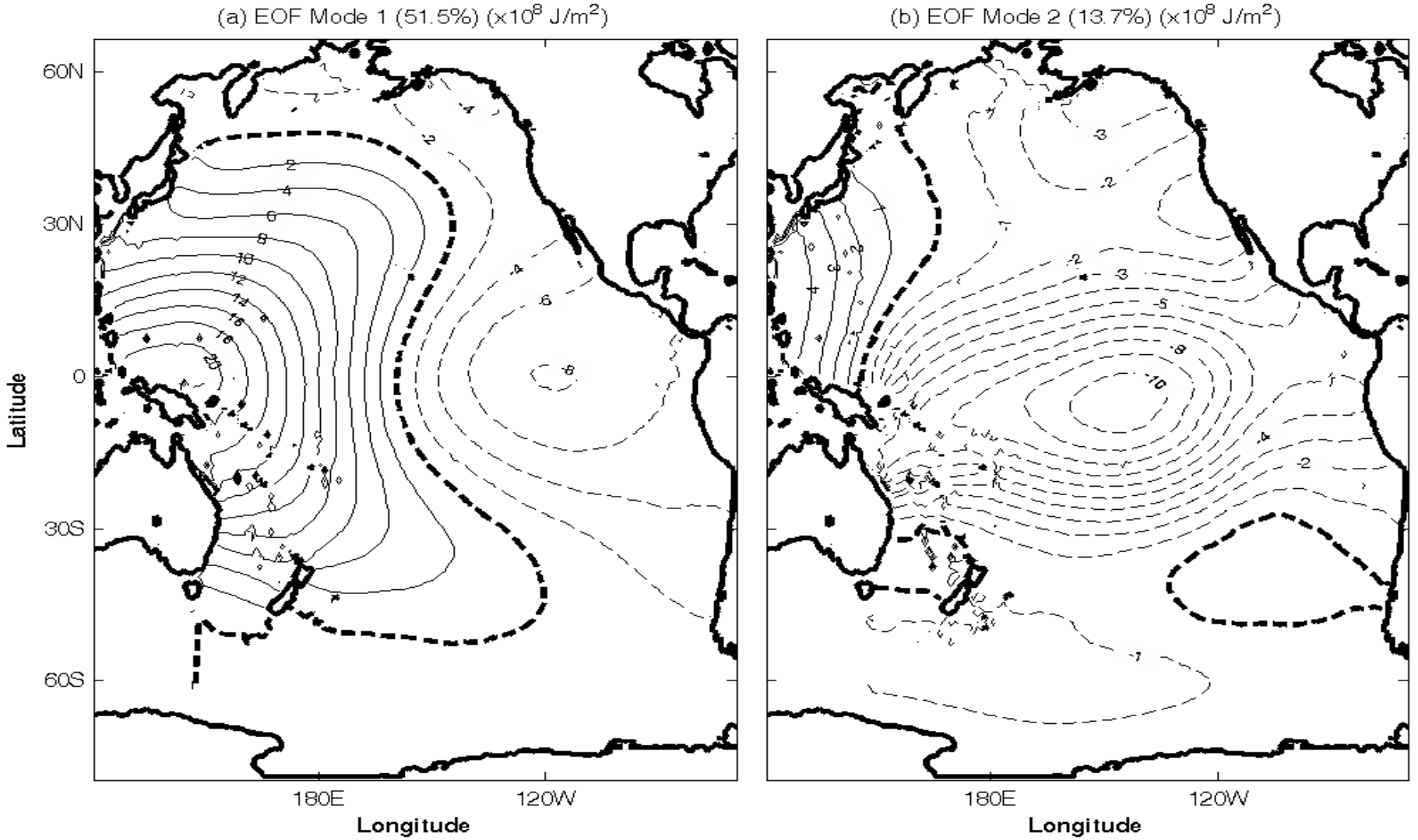
July



October

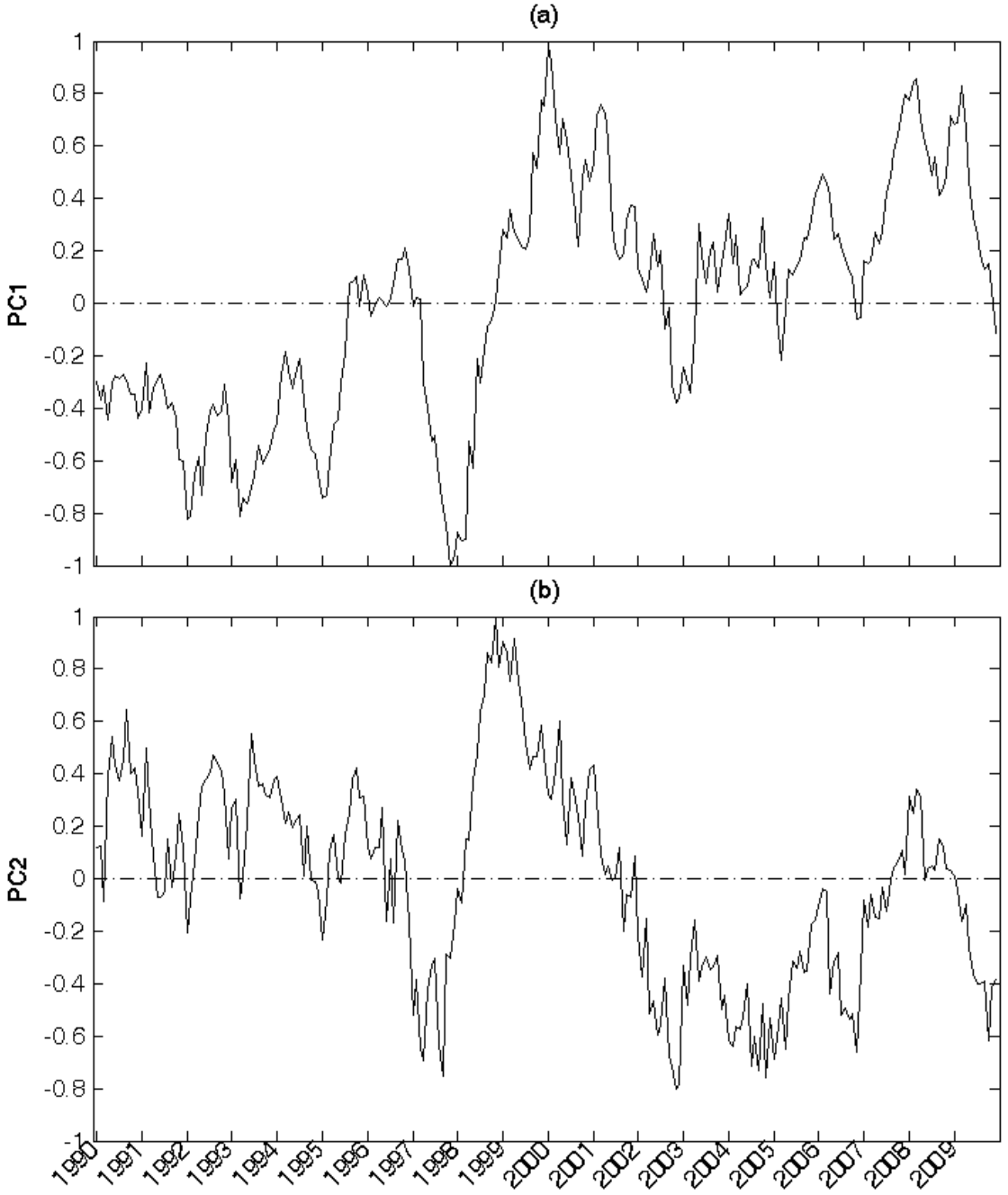


EOF-1 (51.5%) → Canonical El Nino
EOF-2 (13.7%) → El Nino Modoki
Pacific Ocean (in 10^8 J/m^2)



PC1

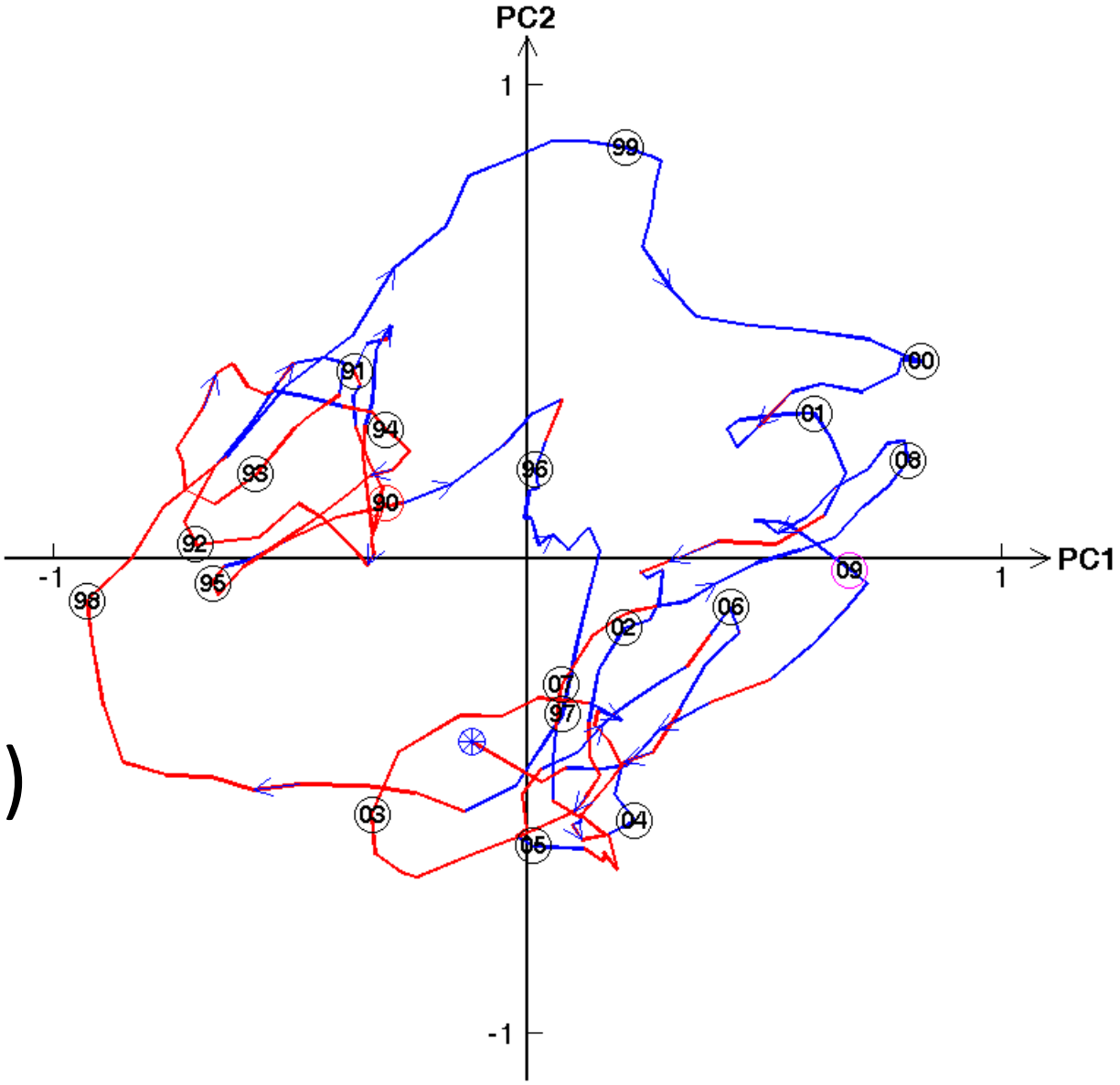
PC2


(a)
PC1
1
0.8
0.6
0.4
0.2
0
-0.2
-0.4
-0.6
-0.8
-1
(b)
PC2
1
0.8
0.6
0.4
0.2
0
-0.2
-0.4
-0.6
-0.8
-1
1990
1991
1992
1993
1994
1995
1996
1997
1998
1999
2000
2001
2002
2003
2004
2005
2006
2007
2008
2009

Phase Diagram (Pacific)

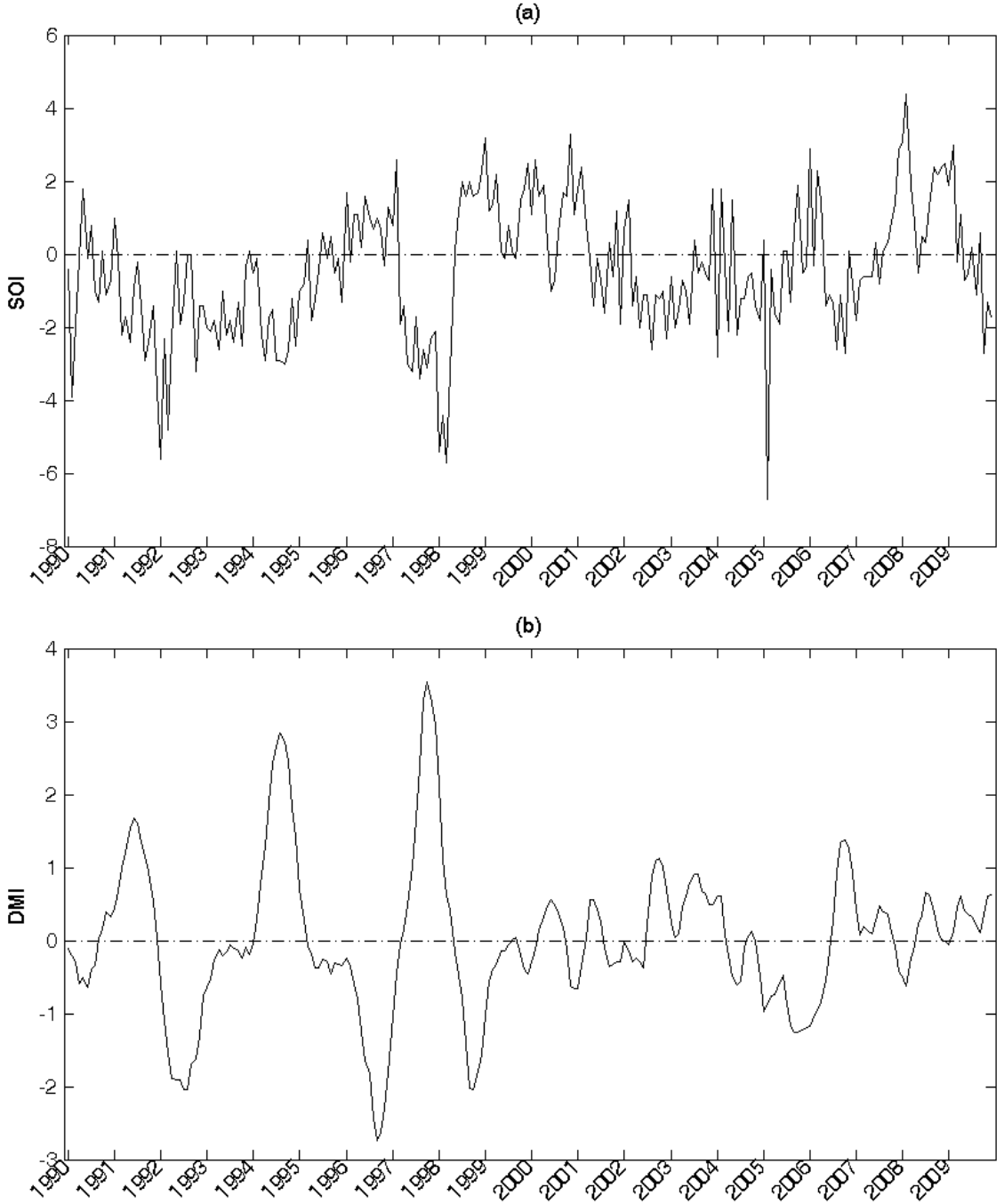
Red → SOI (-)

Blue → SOI (+)



Southern Oscillation Index (SOI)

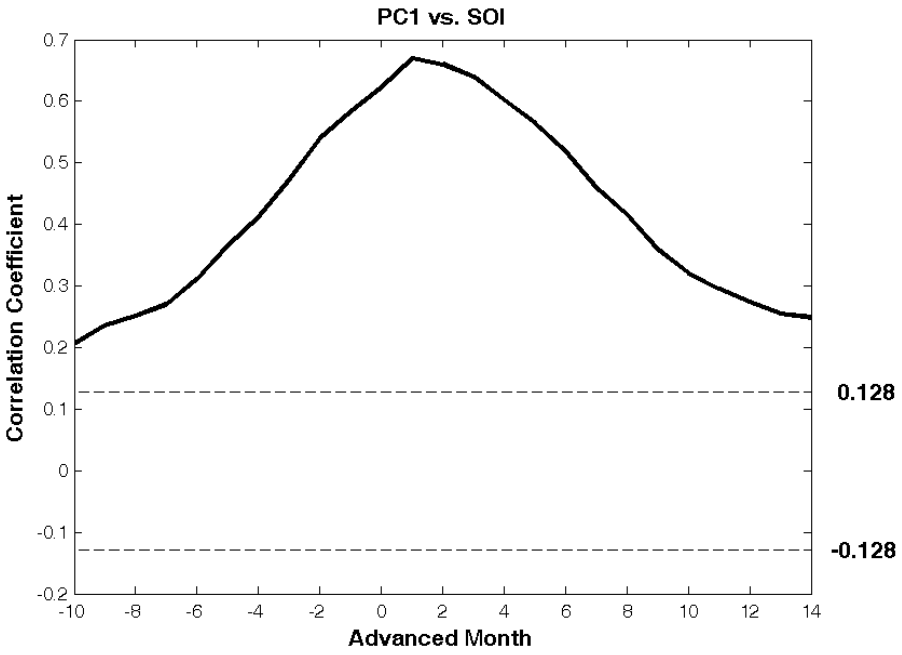
Dipole Mode Index (DMI)

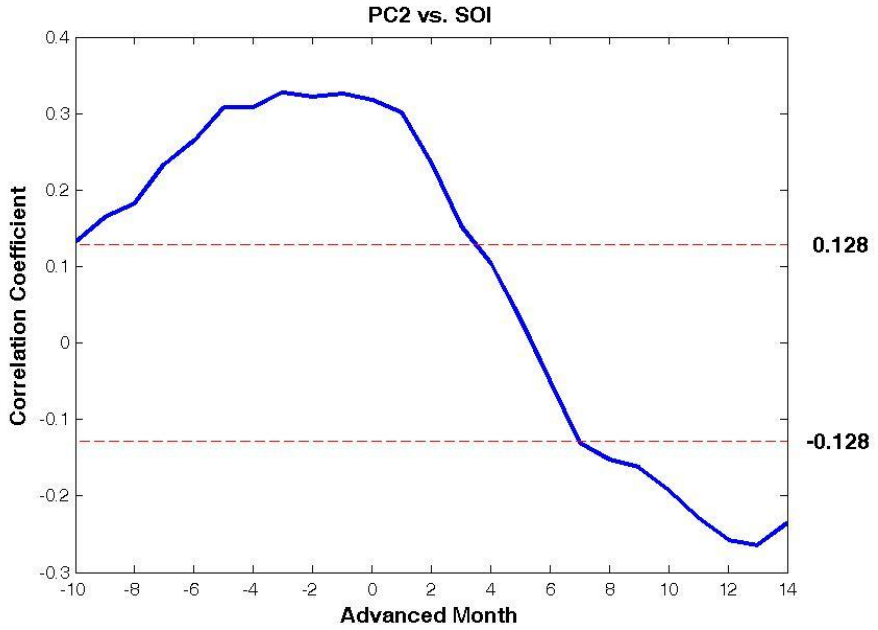


Lag-Correlation Coefficients

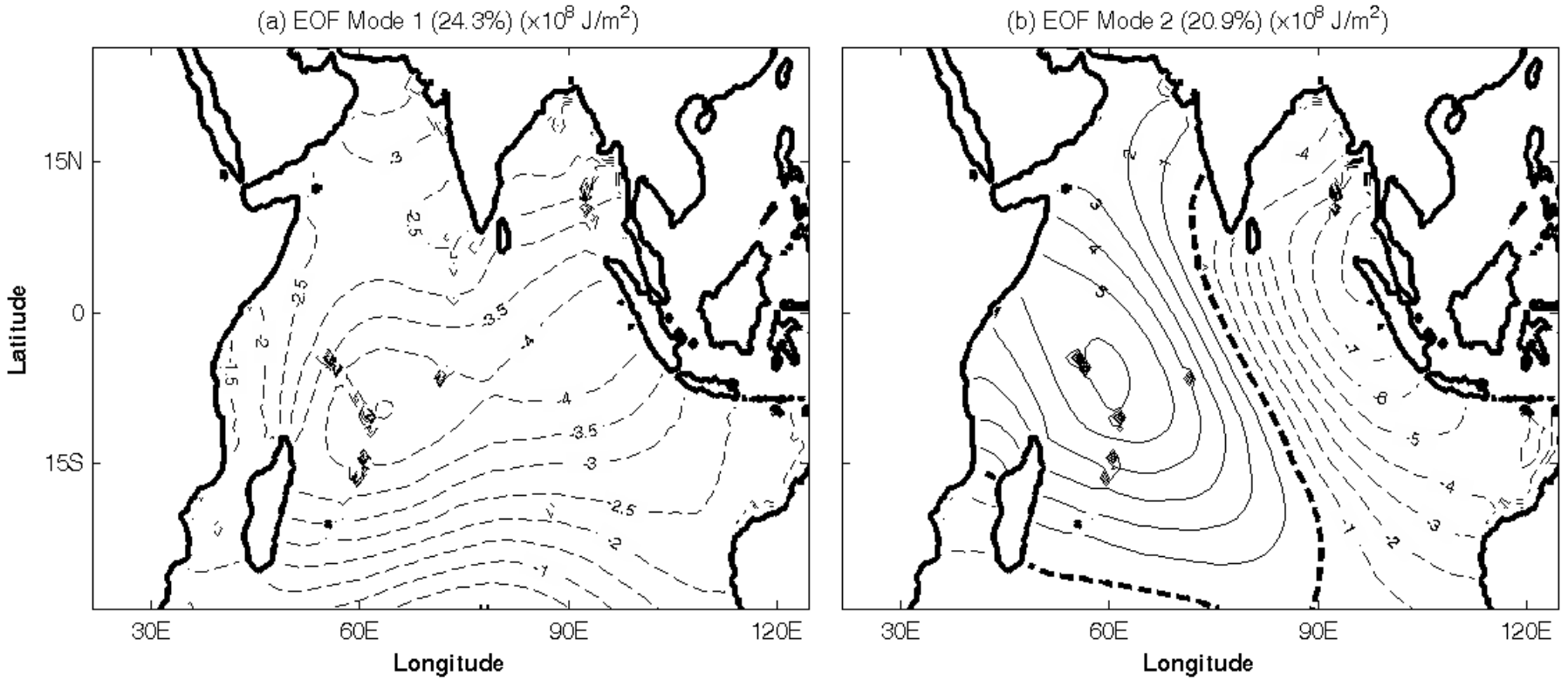
PC1 ←→ SOI

PC2 ←→ SOI





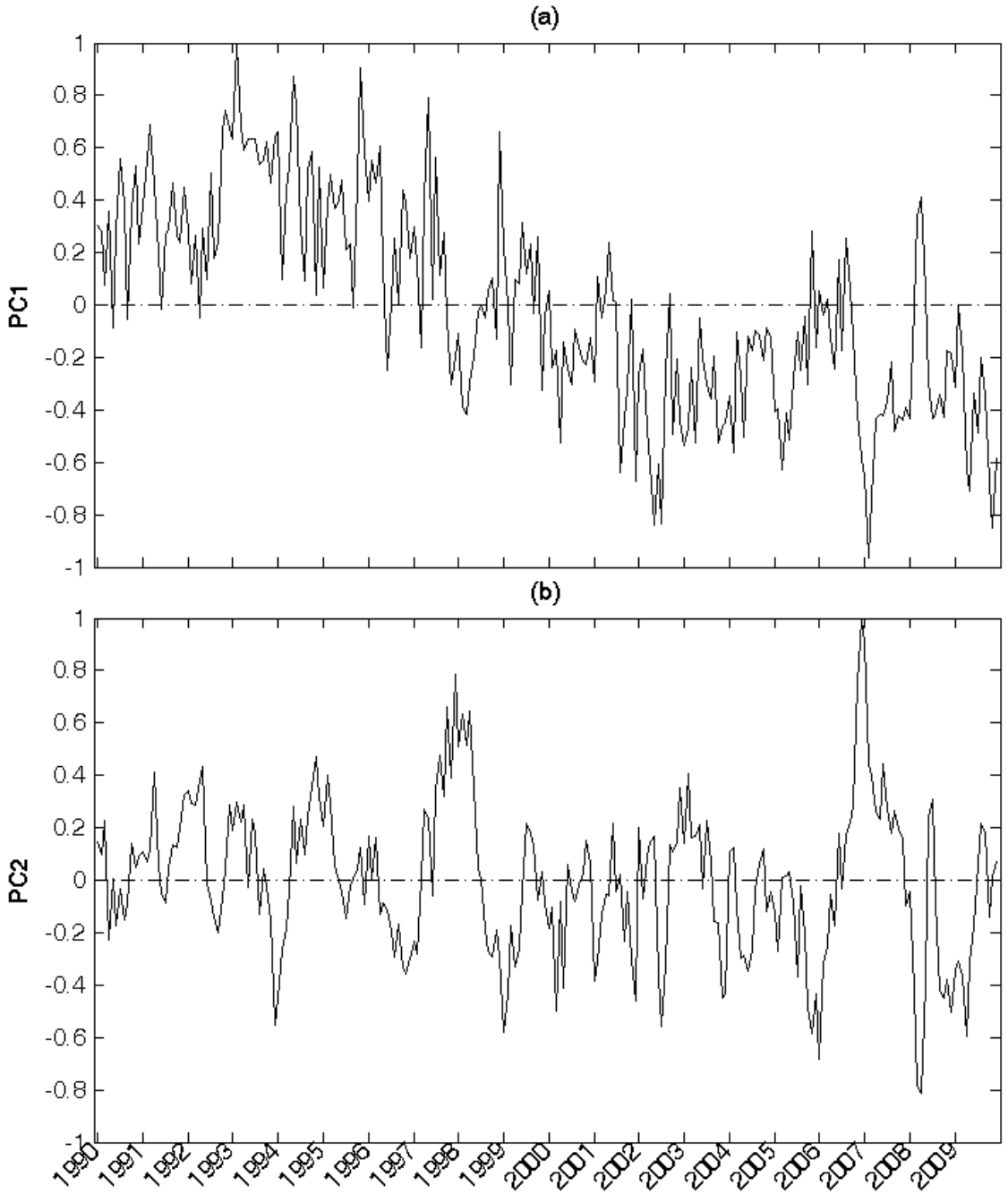
EOF-1 (24.3%) → Basin-scale Oscillation
EOF-2 (20.9%) → Dipole Mode
Indian Ocean (in 10^8 J/m^2)



PC1

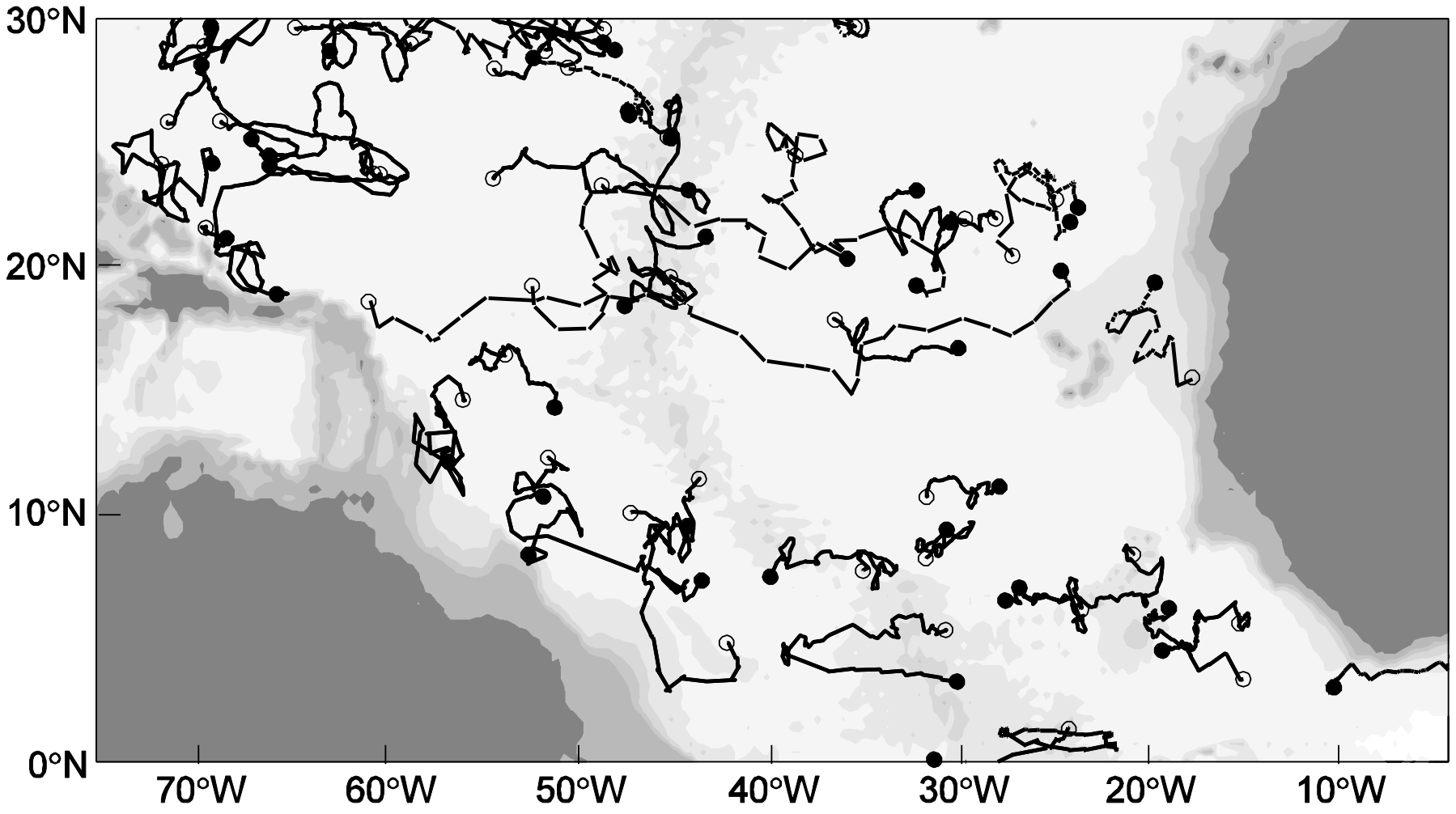
→ Decadal

PC2

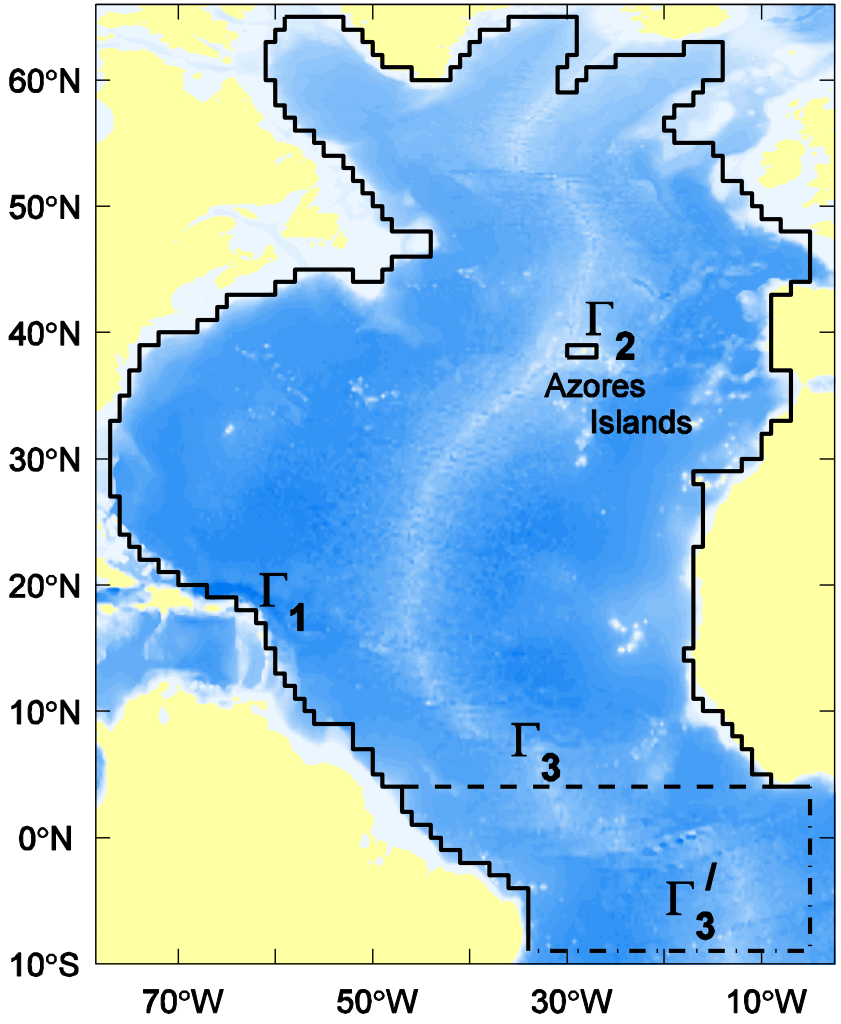


(4) Mid-Depth Rossby wave propagation

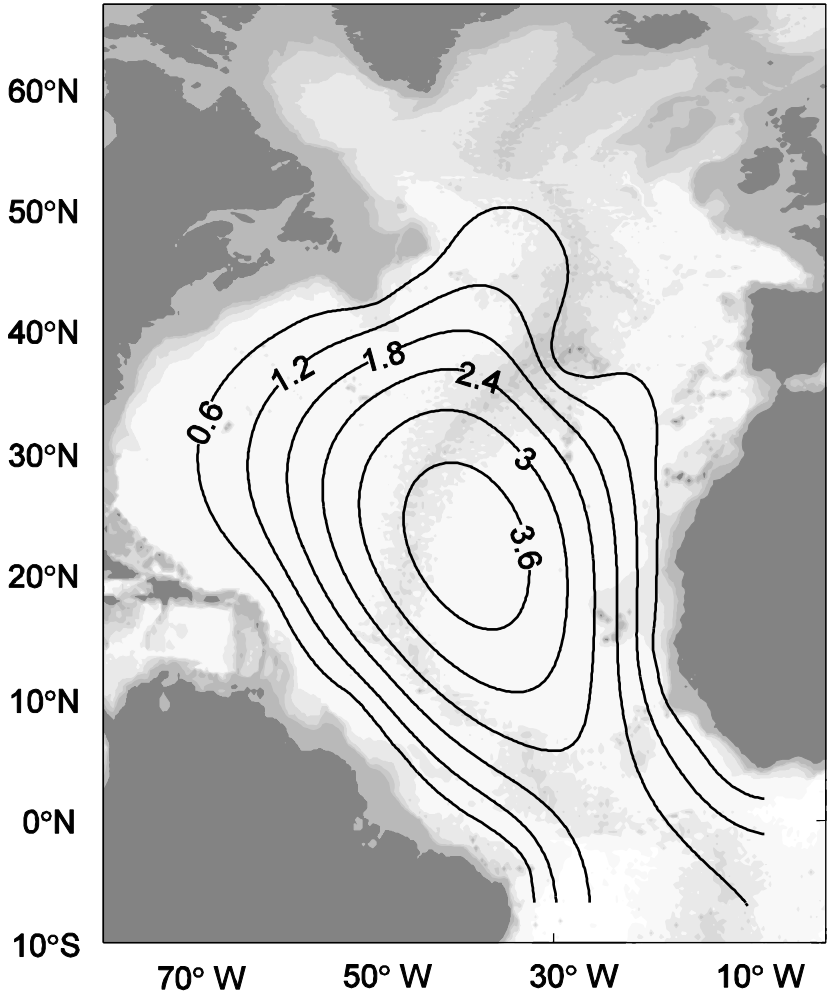
Argo float tracks (with 300 days or longer drifting) at 1000 m and 1500 m (April 04-April 05)

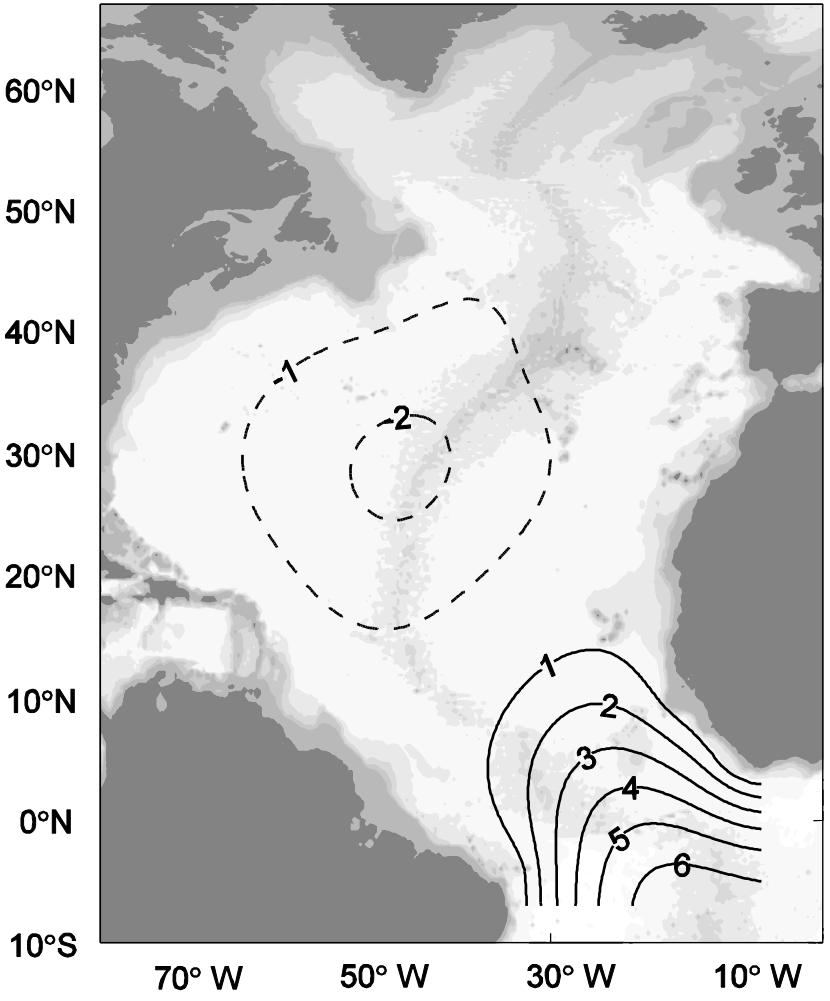


Boundary Configuration → Basis Functions for OSD



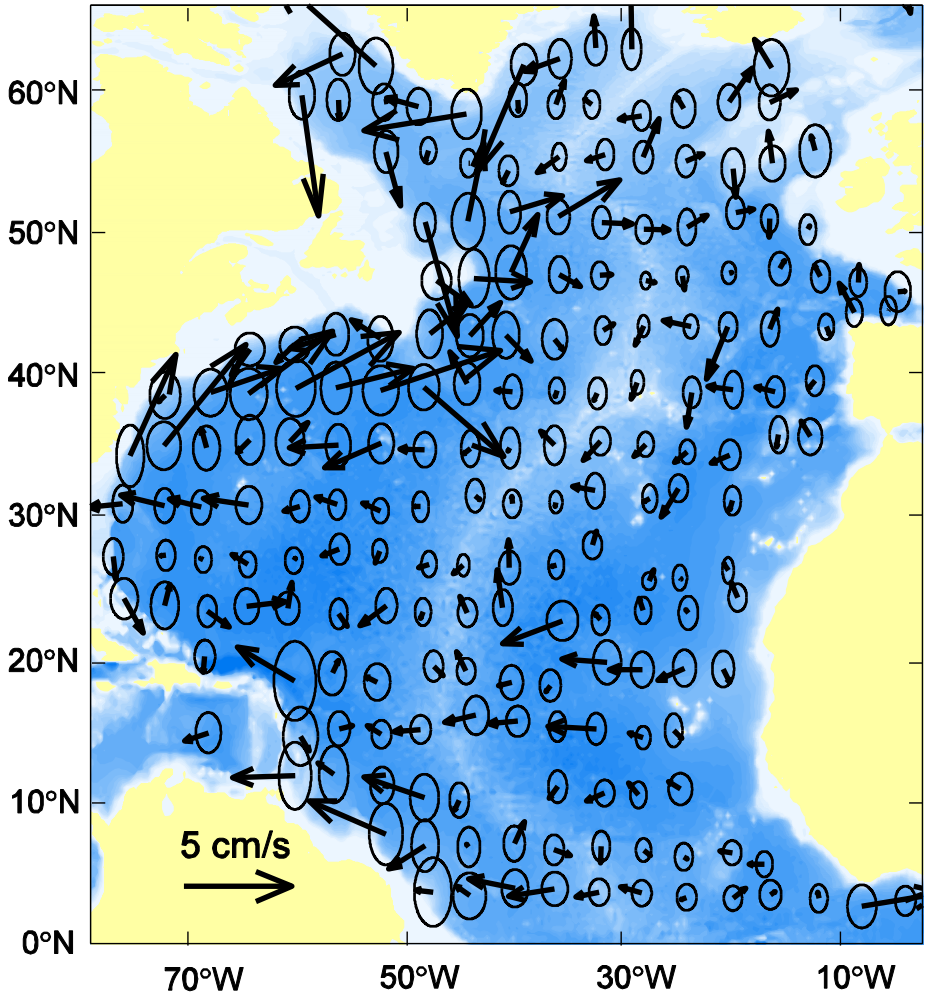
Basis Functions for Streamfunction Mode-1 and Mode-2



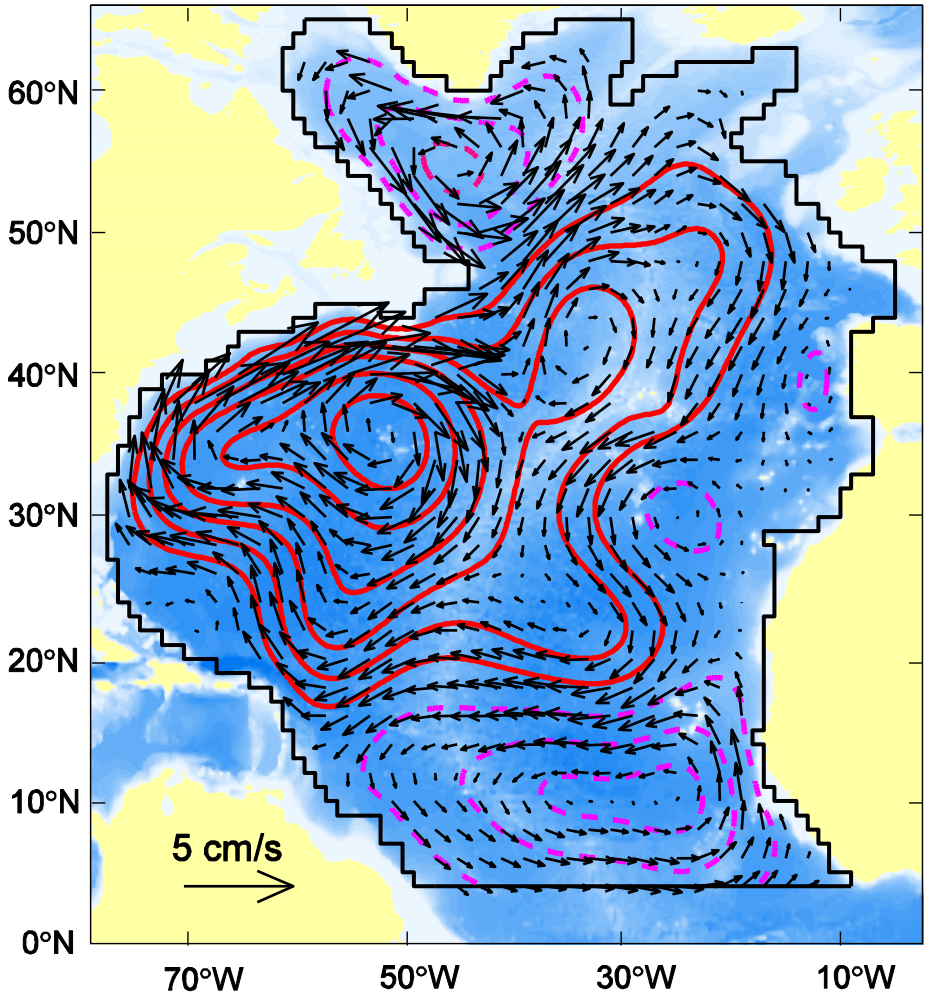


Circulations at 1000 m (March 04 to May 05)

Bin Method



OSD



Correction of Upper Ocean Current Drifting Caused by Vertical Shear

$$\hat{\mathbf{x}}_p = \mathbf{x}_p - \mathbf{U}_p^{eff}\ t_p$$

t_p → ascending/descending time (~ 10 hrs)

$$\mathbf{U}_p^{eff} = \frac{1}{H_p^0} \int_{H_p^0}^{0} \mathbf{U}^*(z)\, dz$$

$$\mathbf{U}^* = -(\mathbf{U}_{surf} - \mathbf{U}_{now}) \frac{(z - H_p^0)}{H_p^0} + \mathbf{U}_{now}$$

Fourier Expansion → Temporal Annual and Semi-anuual

$$\hat{T}(\mathbf{x}_\perp, z, t) \approx \overline{T}(\mathbf{x}_\perp, z) + T_1(\mathbf{x}_\perp, z, t) + T_2(\mathbf{x}_\perp, z, t),$$

$$T_1(\mathbf{x}_\perp, z, t) = \sum_{m=1}^{M_{opt}} C_{\omega_1, m}(z) \cos[\omega_1 t + \chi_{\omega_1, m}(z)] \Xi_m(\mathbf{x}_\perp, z),$$

$$T_2(\mathbf{x}_\perp, z, t) = \sum_{m=1}^{M_{opt}} C_{\omega_2, m}(z) \cos[\omega_2 t + \chi_{\omega_{21}, m}(z)] \Xi_m(\mathbf{x}_\perp, z),$$

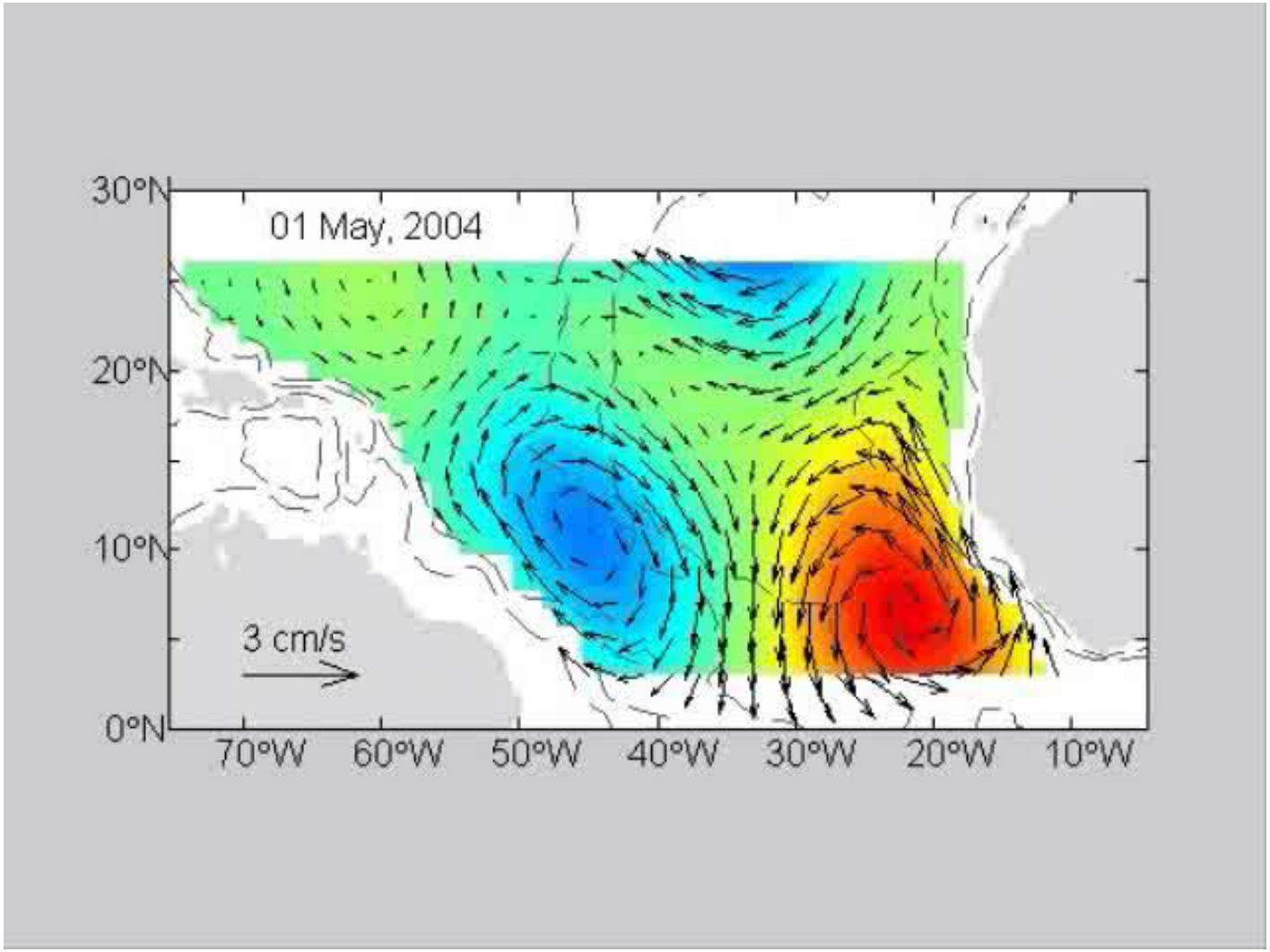
T_0=12 months; $\omega_1 = 2\pi / T_0$; $\omega_2 = 4\pi / T_0$

Optimization

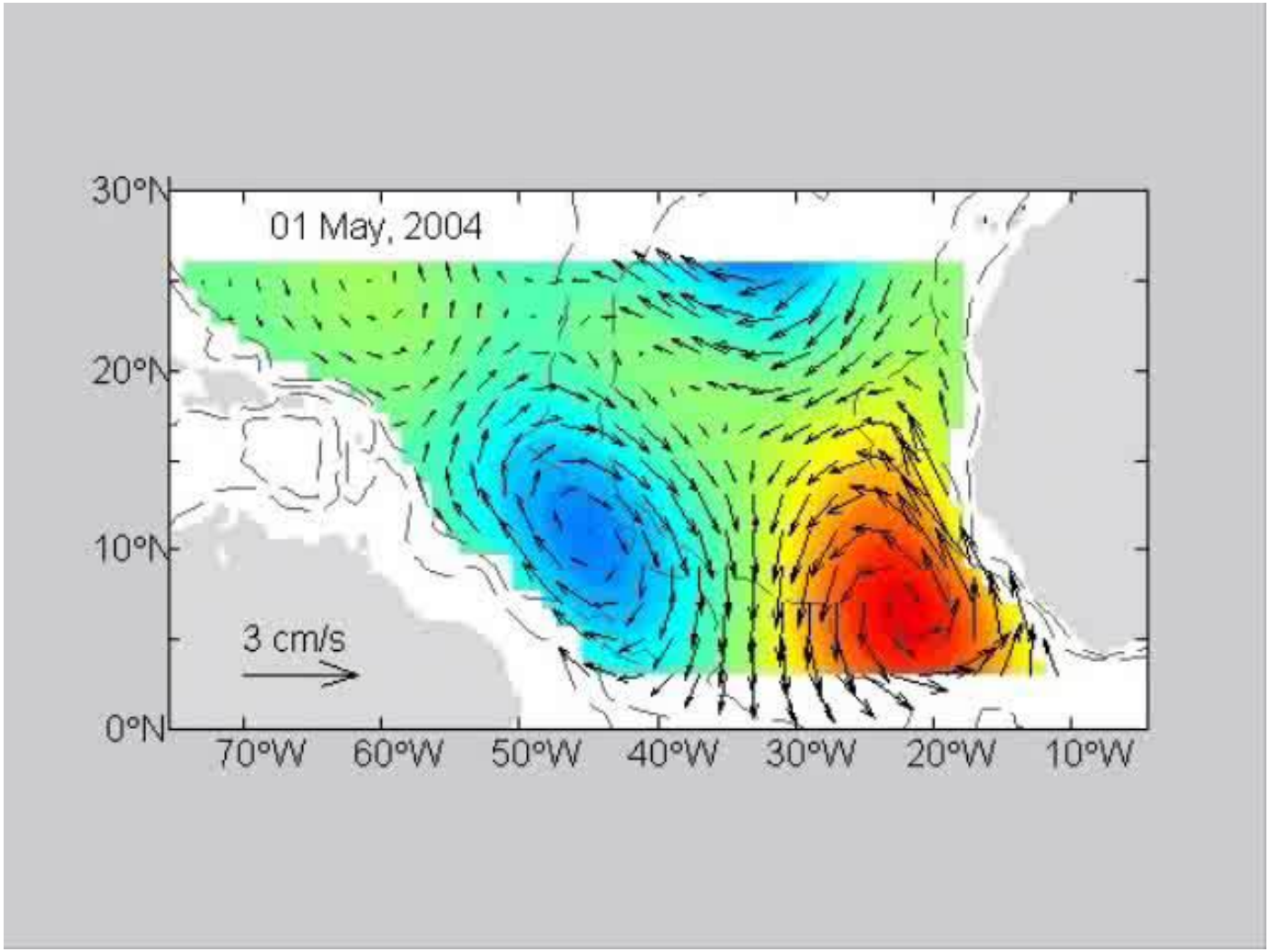
$$J_s = \int_{t_o}^{t_o+T_o} \left[a_s(t) - \sum_{\omega=\omega_1,\omega_2} A_{\omega,s} \cos(\omega t + \theta_{\omega,s}) \right]^2 dt \rightarrow \min$$

$$I_k = \int_{t_o}^{t_o+T_o} \left[b_k(t) - \sum_{\omega=\omega_1,\omega_2} B_{\omega,s} \cos(\omega t + \vartheta_{\omega,s}) \right]^2 dt \rightarrow \min$$

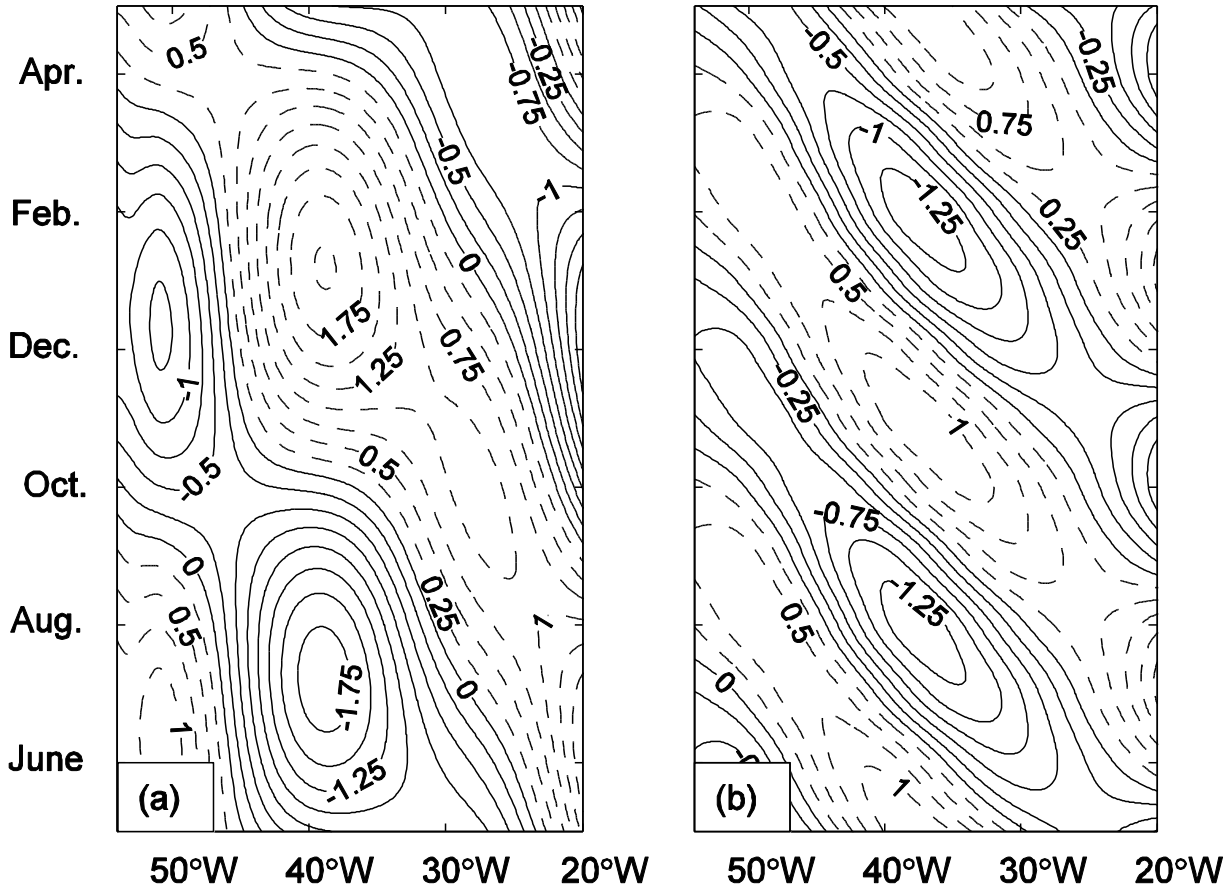
Annual Component



Semi-annual Component



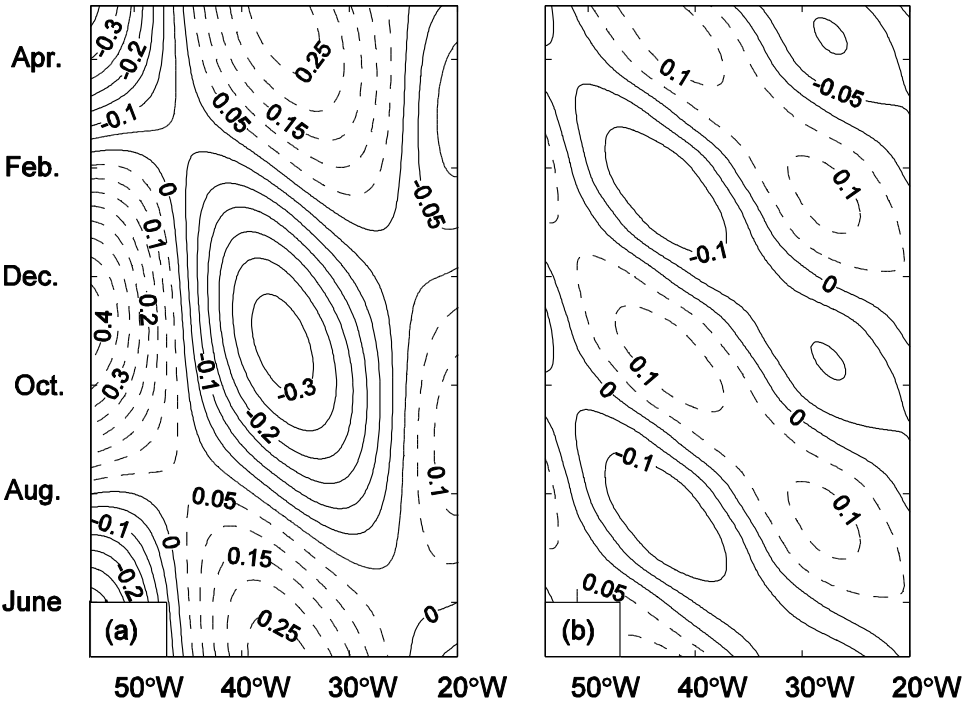
Time –Longitude Diagrams of Meridional Velocity Along 11°N



Annual

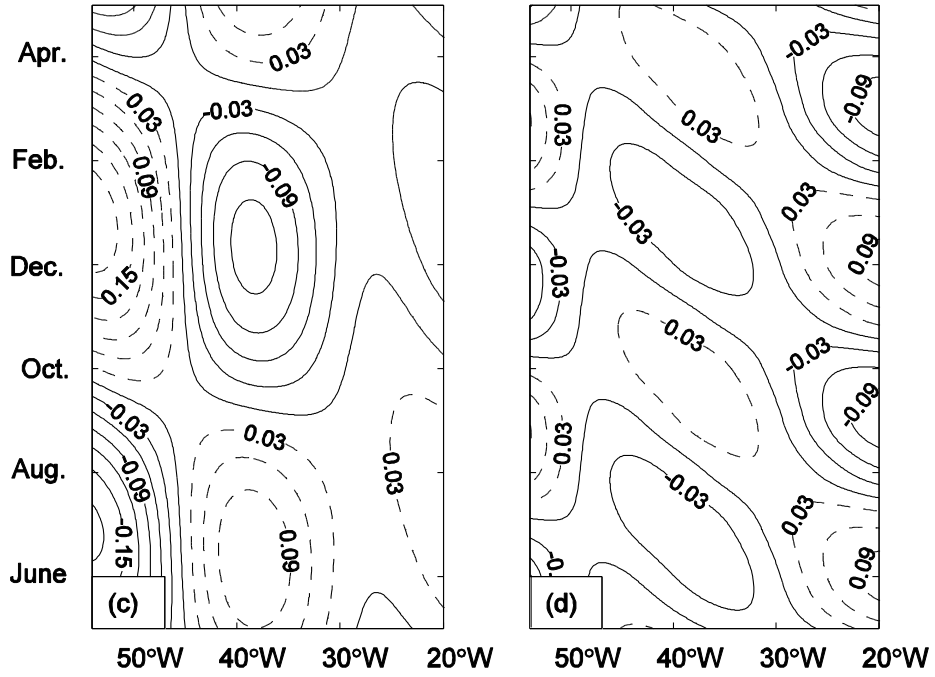
Semi-Annual

Time –Longitude Diagrams of temperature Along 11°N



Annual

Semi-Annual



Annual

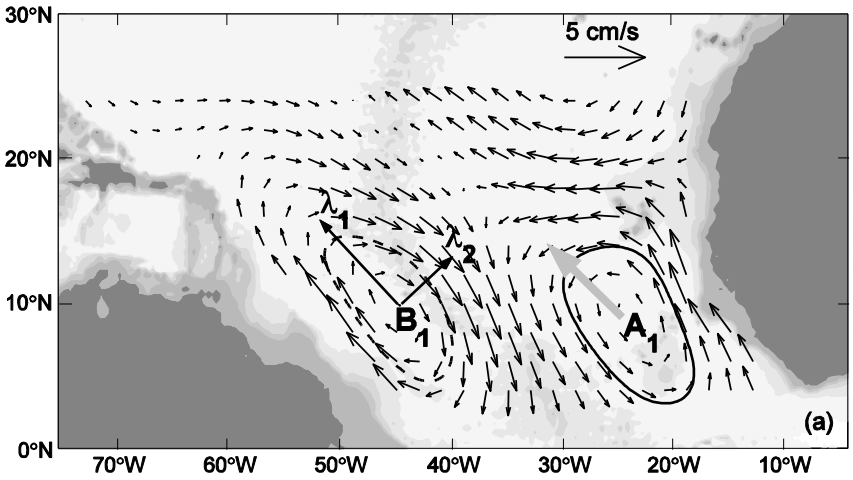
Semi-Annual

550 m

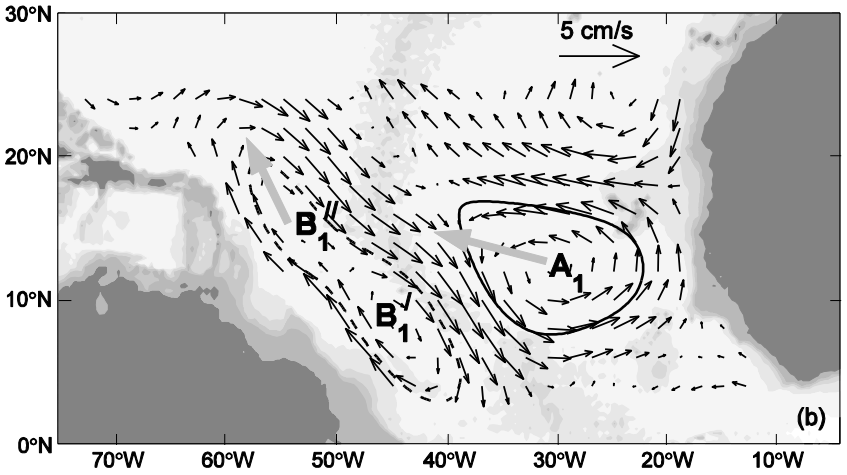
950 m

Annual Currents (1000 m)

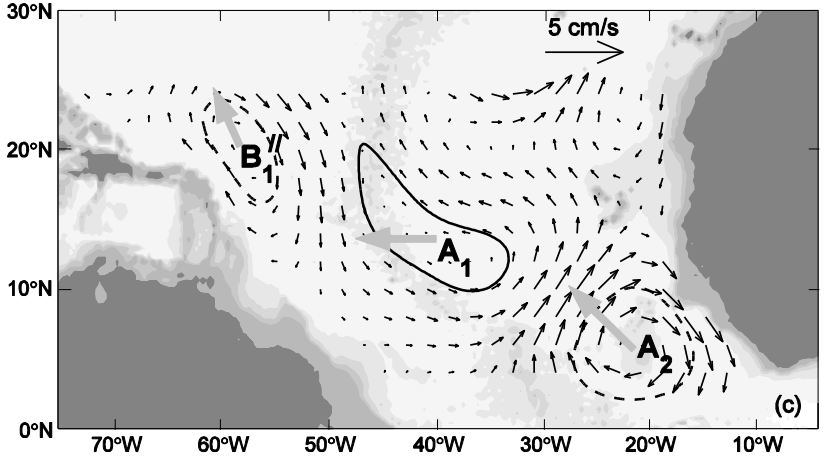
May-Jun 2004



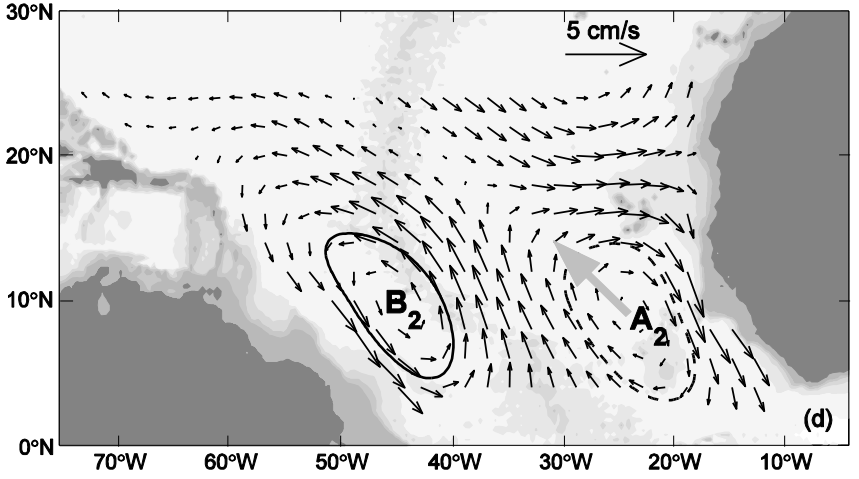
Jul-Aug 2004



Sep-Oct 2004



Nov-Dec 2004



Characteristics of Annual Rossby Waves

	March, 04 – May, 05 float data			March, 04 – May, 06 float data		
Latitude	c_p (cm/s)	L_1 (km)	L_2 (km)	c_p (cm/s)	L_1 (km)	L_2 (km)
5^0N	12	1200	1100	12	1300	900
8^0N	16	2500	1400	12	2100	1100
11^0N	14	2200	1400	11	1900	1100
13^0N	11	2100	1500	10	2300	1500

Western Basin

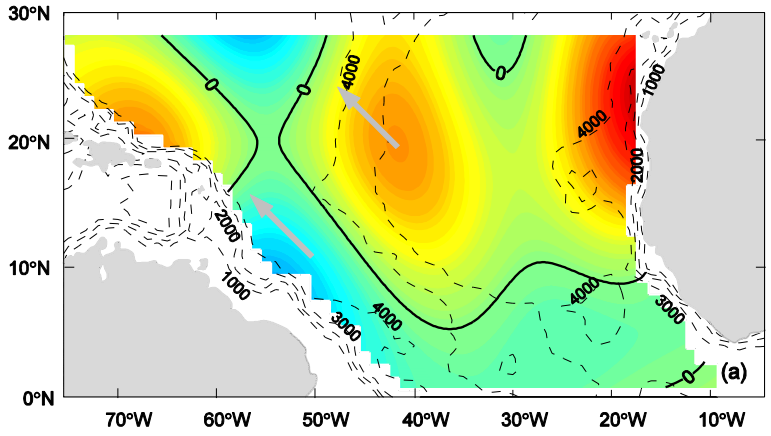
Eastern Basin

Western Basin

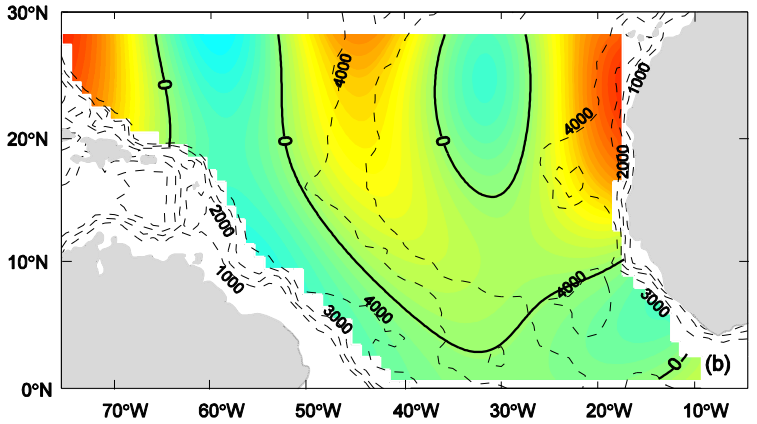
Eastern Basin

Annual Monthly Temperature Anomaly (°C) at 950 m Depth → Annual Rossby Waves (7-10 cm/s)

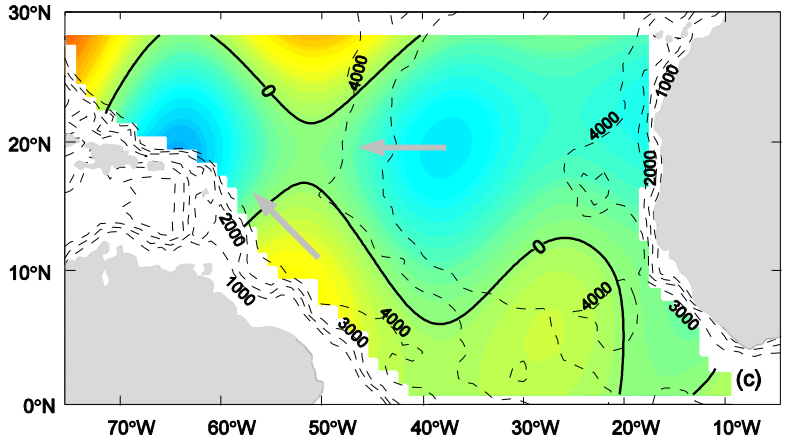
Jun 04



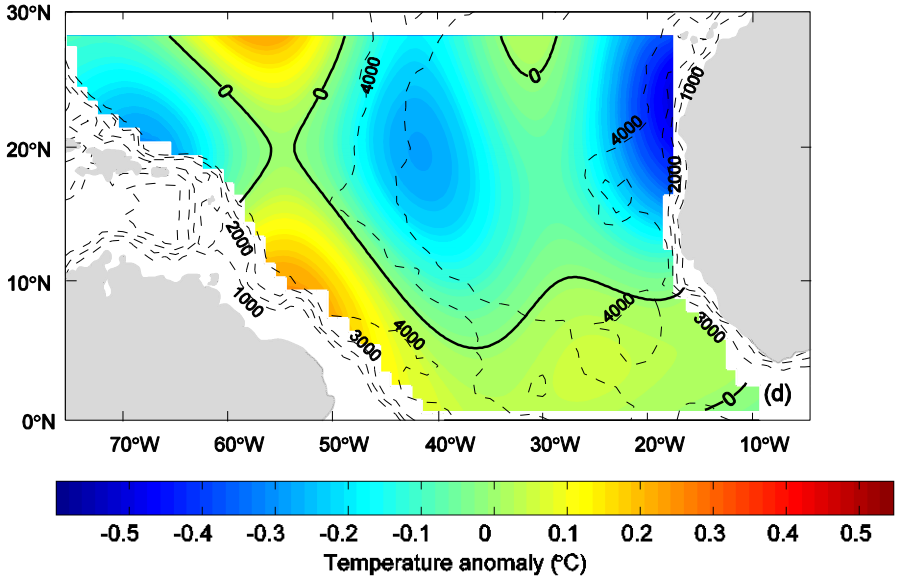
Aug 04



Oct 04

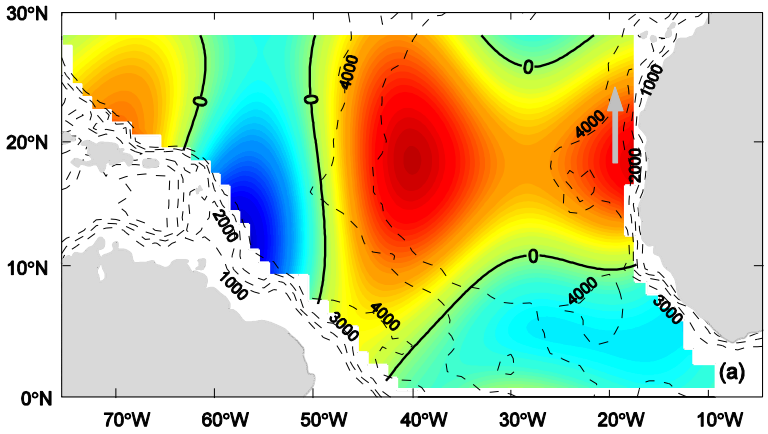


Dec 04

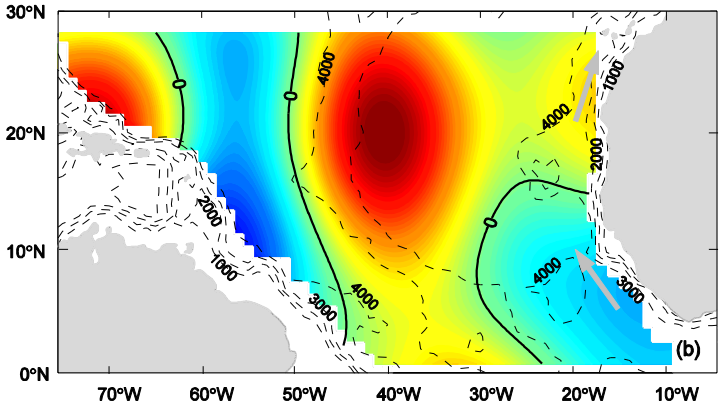


Annual Monthly Temperature Anomaly (°C) at 250 m Depth → Equatorially Forced Coastal Kelvin waves (27-30 cm/s)

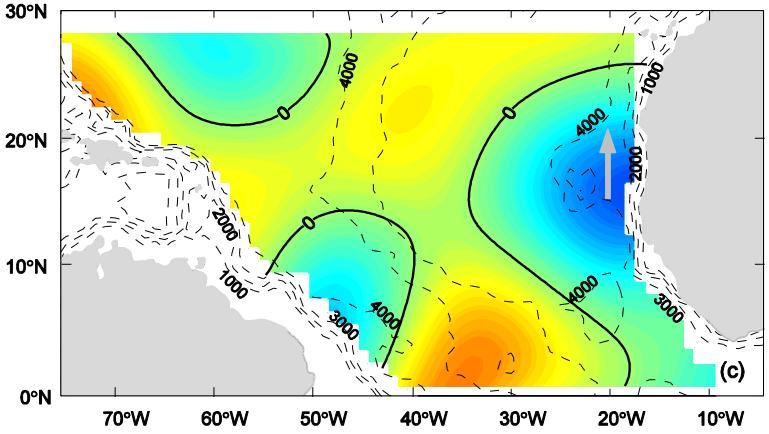
Jun 04



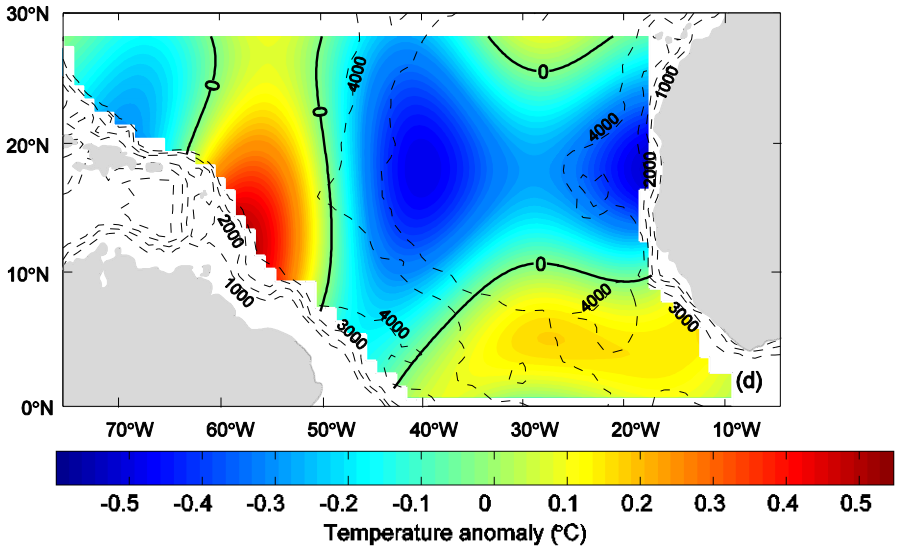
Aug 04



Oct 04

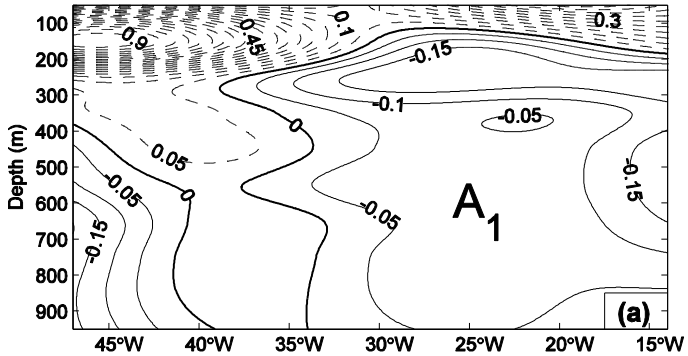


Dec 04

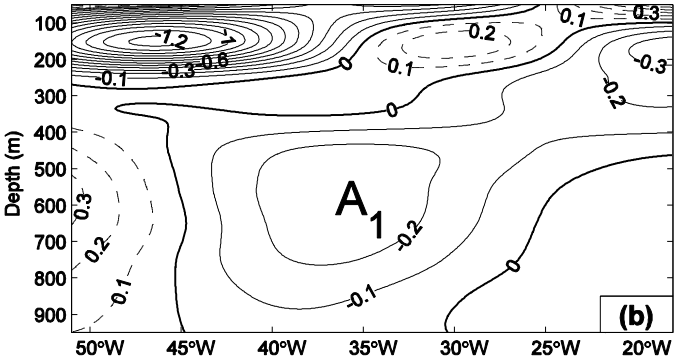


Zonal cross-sections of the annual component of the temperature anomaly (°C)

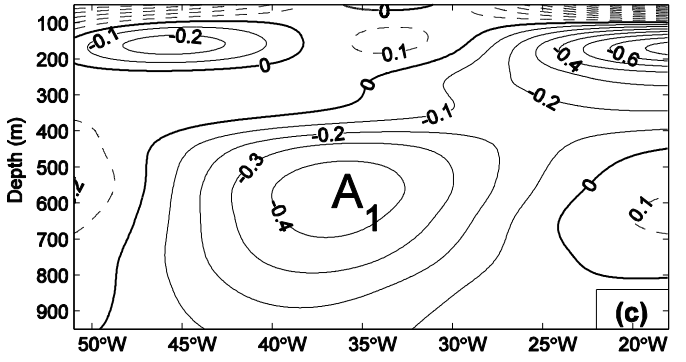
6°N in Jun 04 →



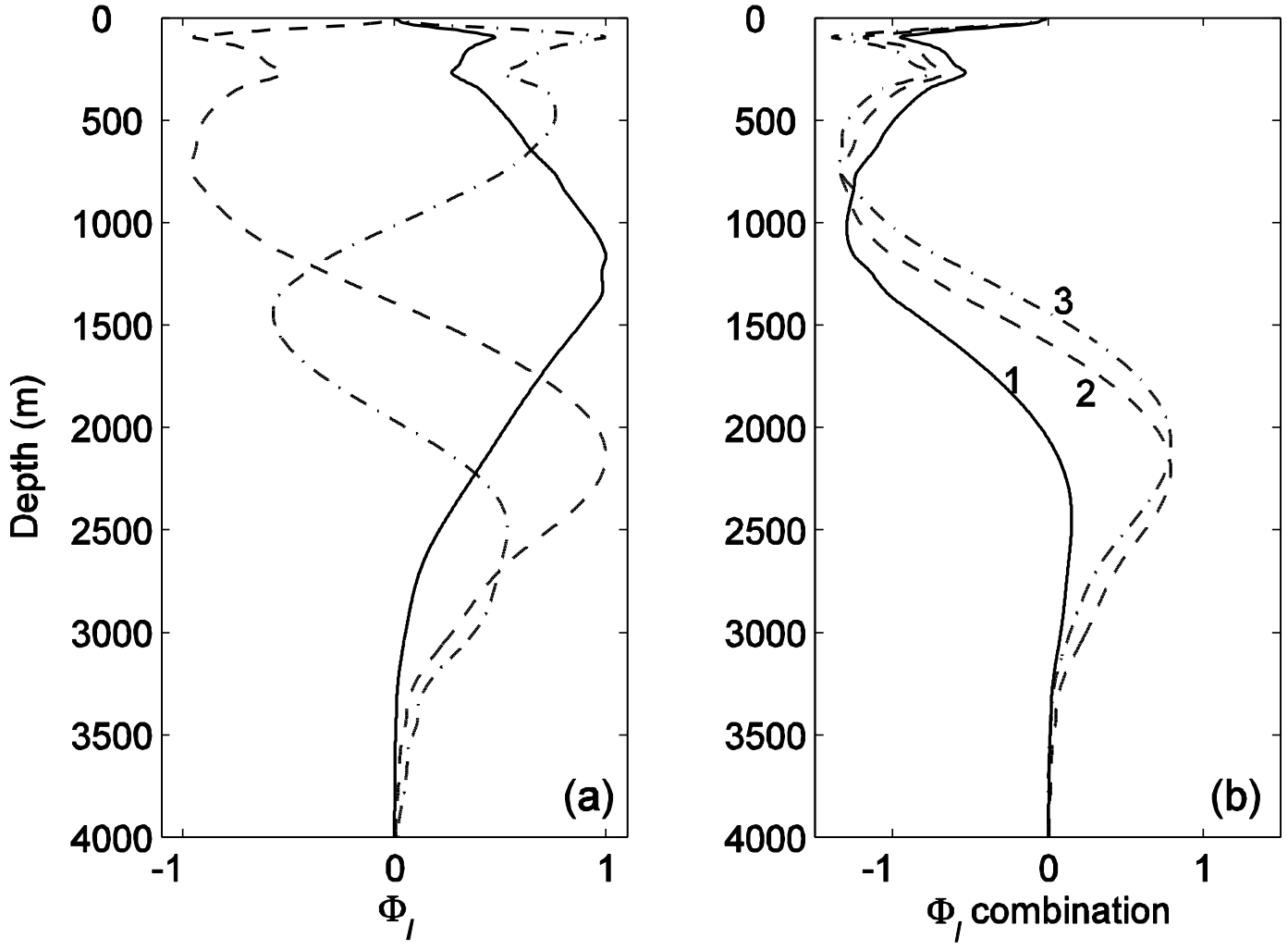
11°N in Oct, 04 →



16°N in Oct 04 →



Baroclinic Modes



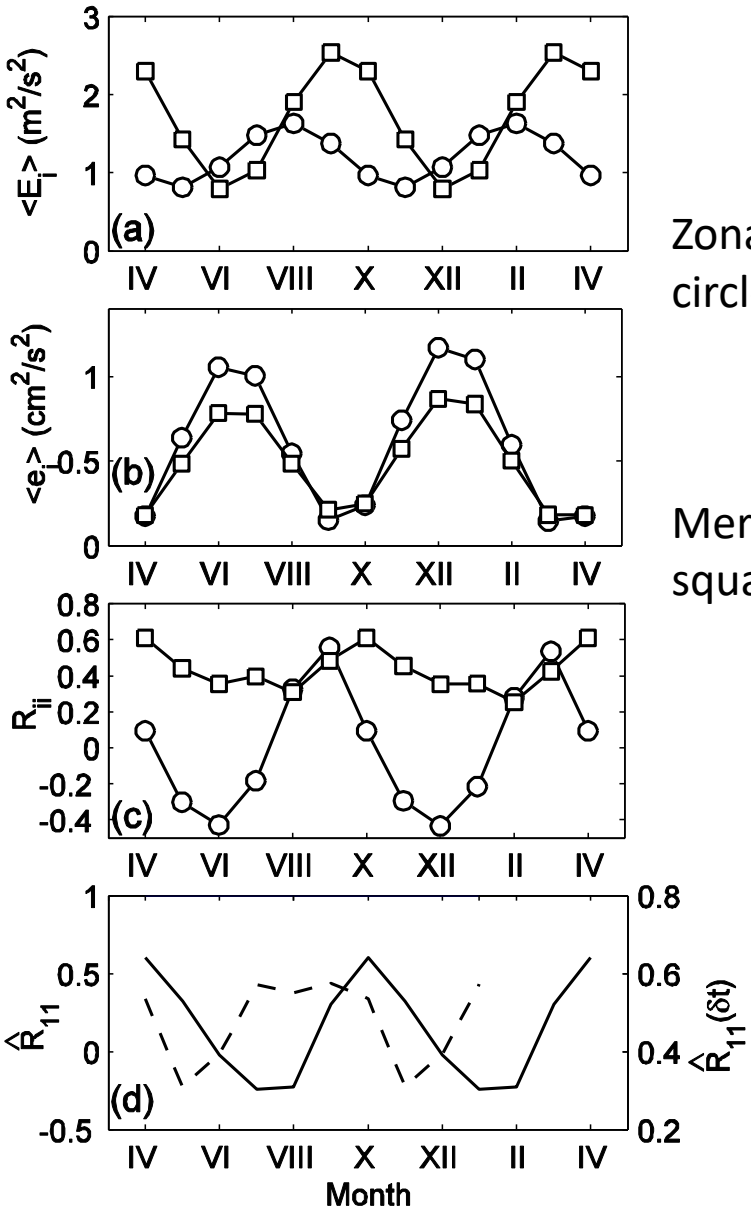
Annual Component in the Western Sub-Basin

Mean wind KE

Mean KE for mid-depth currents

Correlation between Winds and currents

Correlation between wind Stress curl and streamfunction (solid: no-lag, dashed: 3 mon lag



Zonal: circle

Meridional: square

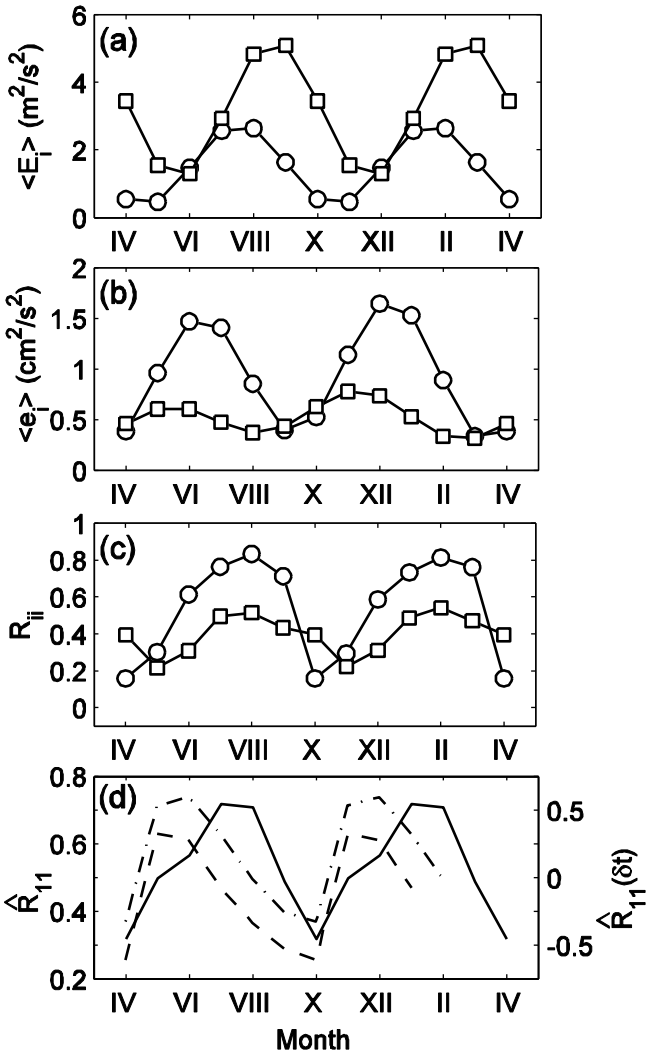
Annual Component in the Eastern Sub-Basin

Mean wind KE

Mean KE for mid-depth currents

Correlation between Winds and currents

Correlation between wind Stress curl and streamfunction (solid: no-lag, dashed: 3 mon lag

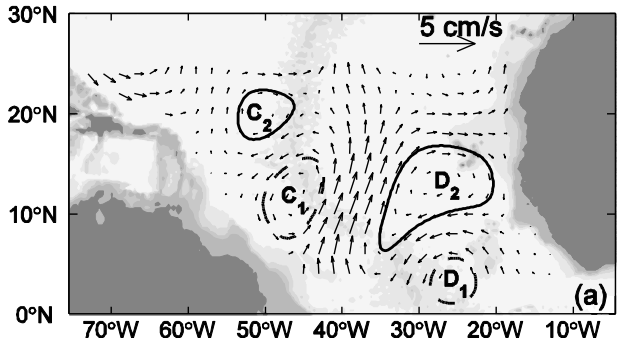


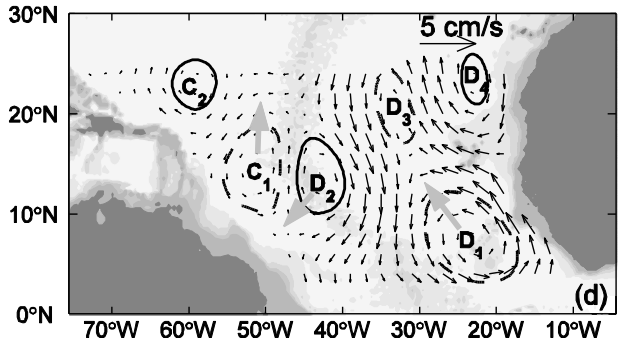
Zonal: circle

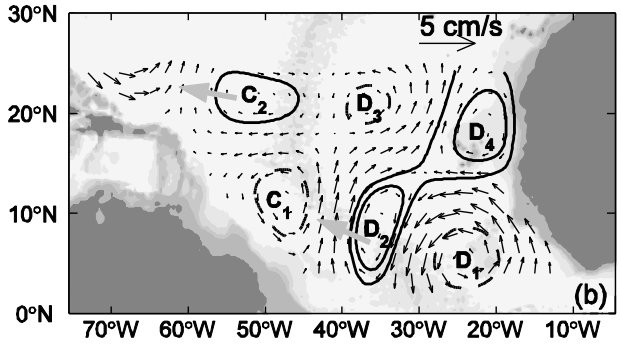
Meridional: square

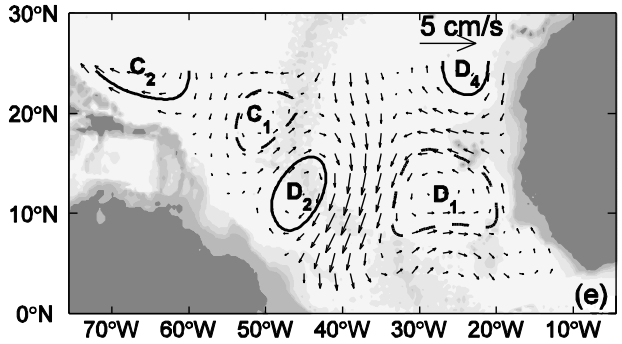
Semi-annual currents at 1000 m depth (2004)

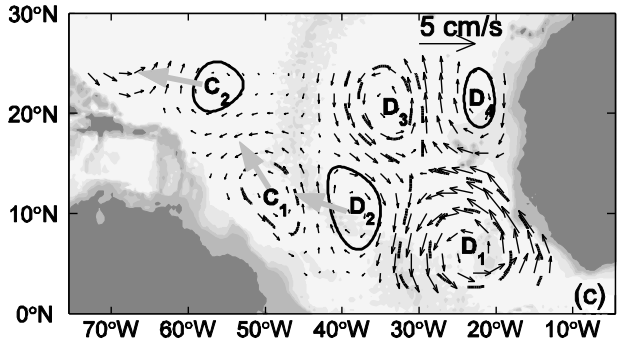
(a)5/15
(b)5/30
(c)6/14
(d)6/29
(e) 7/13





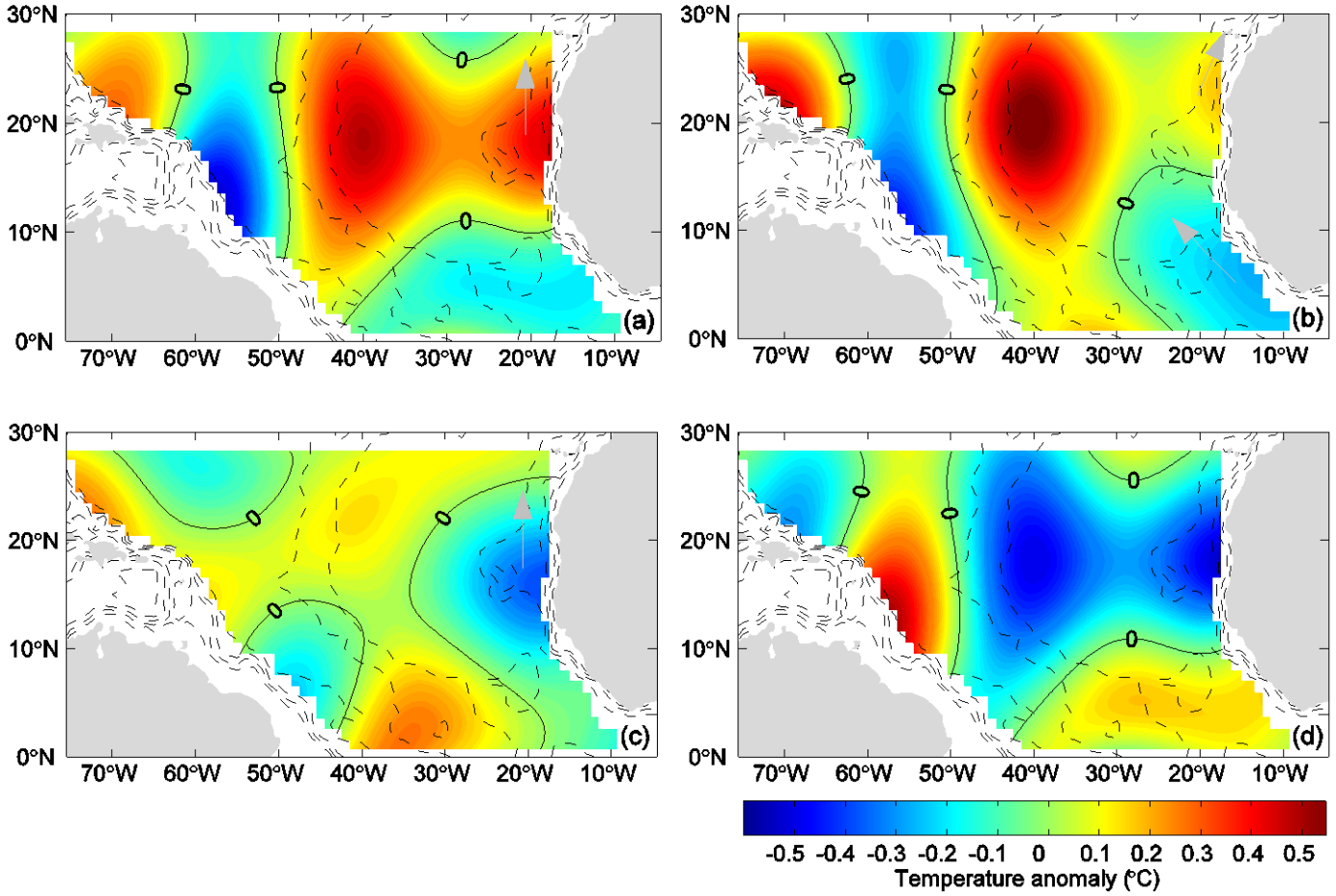






Semi-annual monthly temperature anomaly at 950m depth

(a)Jun 04
(b) Aug 04
(c) Oct 04
(d) Dec 04.



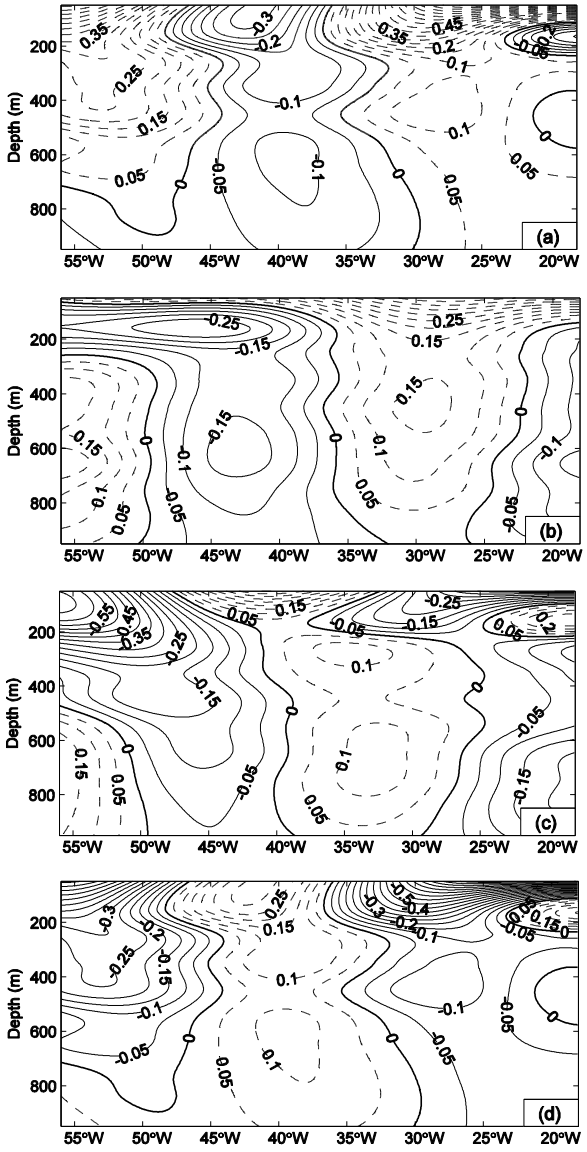
Semi-annual component of monthly temperature anomaly along 11°N (2004)

(a) 6/4

(b) 7/4

(c) 8/4

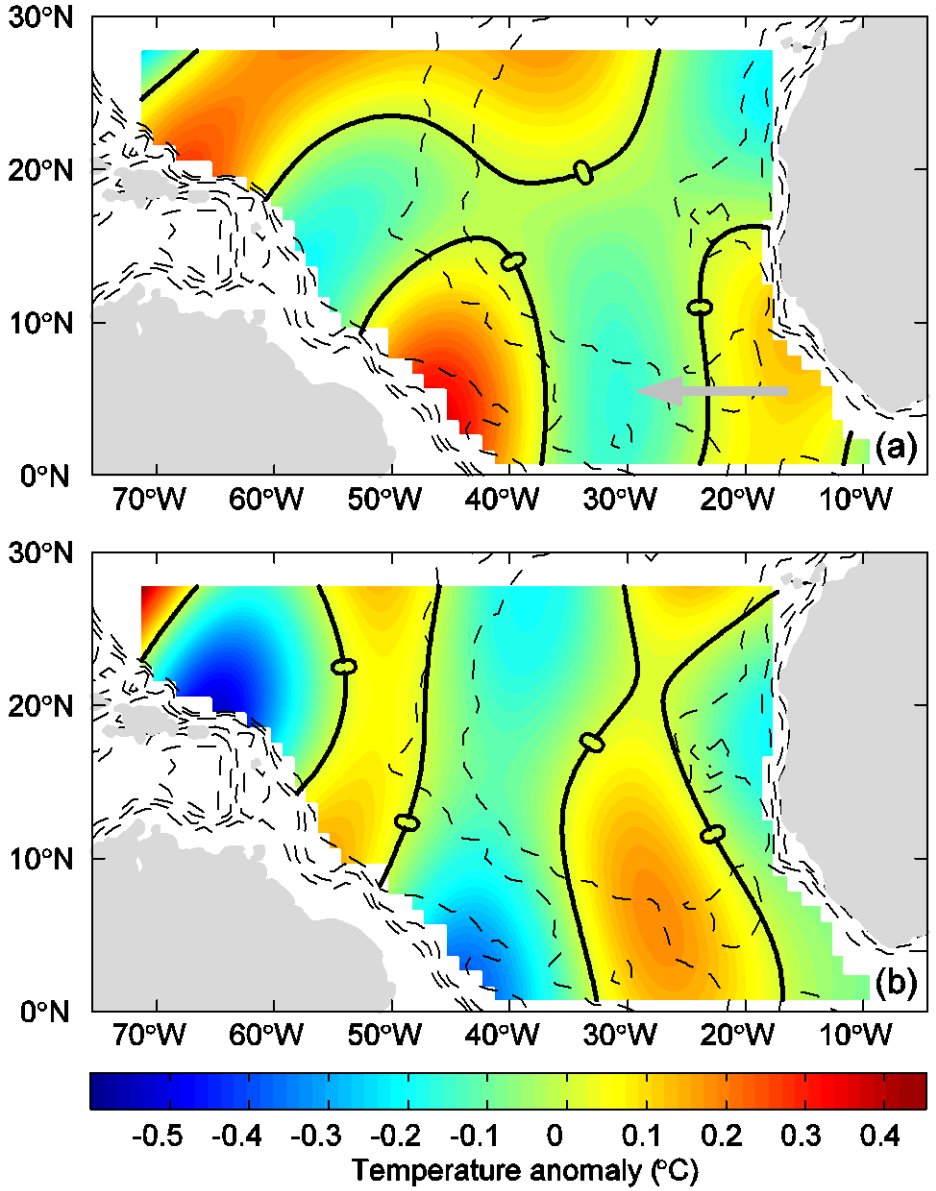
(d) 9/4



Semi-annual temperature anomaly at 550m depth (2004)

(a) 5/15

(b) 6/29



Semiannual Component in the Western Sub-Basin

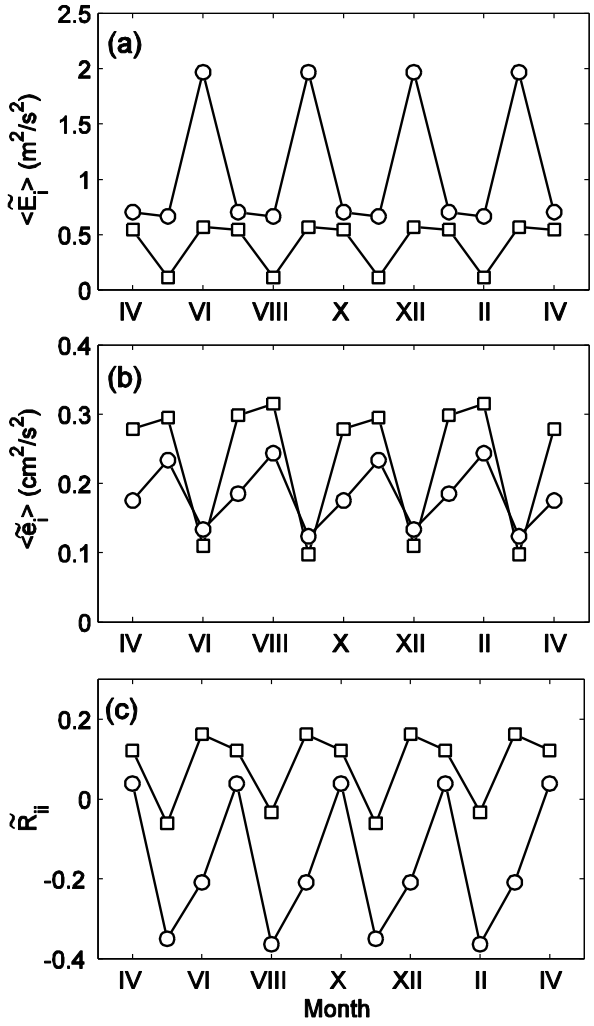
(a) wind KE

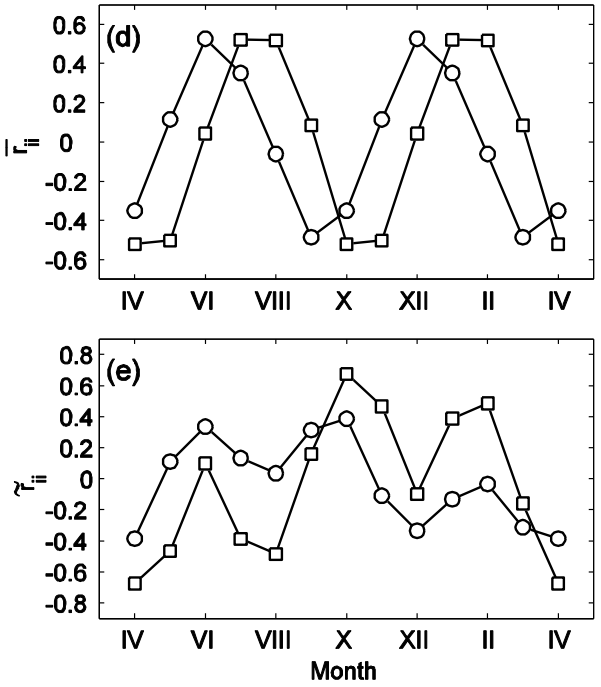
(b) current KE

(c) corr wind stress and currents

(d) corr between semi-annual currents and annual mean wind

(e) corr between semiannual currents and annual wind stress.





Semiannual Component in the Eastern Sub-Basin

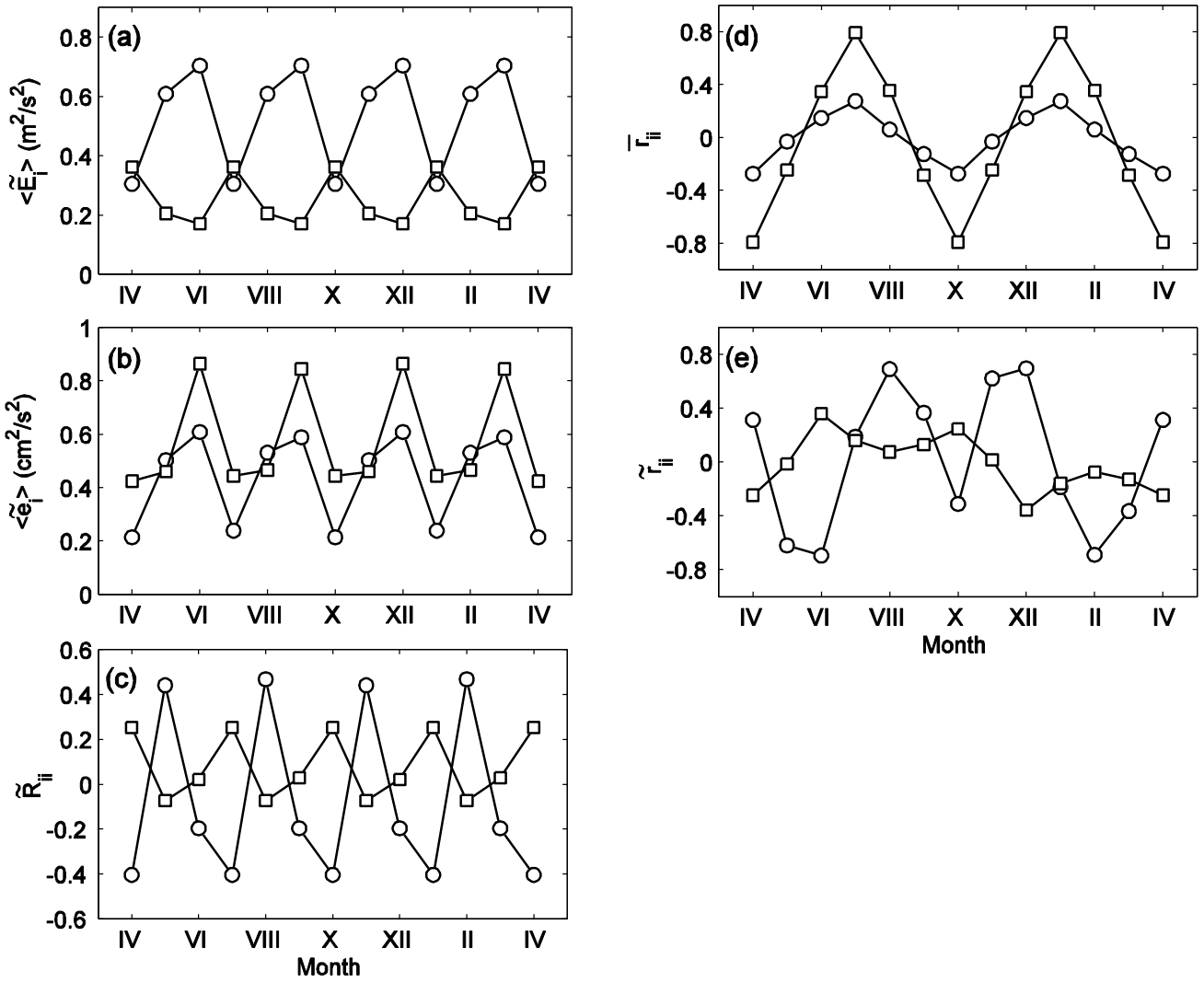
(a) wind KE

(b) current KE

(c) corr wind stress and currents

(d) corr between semi-annual currents and annual mean wind

(e) corr between semiannual currents and annual wind stress.



Results

- Mid-depth Rossby waves are identified using the Argo data.
- The annual and semi-annual Rossby waves are detected in both the western and eastern sub-basins.
- The wind-driven Ekman pumping seems to be responsible for the Rossby wave generation in both the sub-basins.
- Along-shore wind fluctuations and equatorially forced coastal Kelvin waves are found to be responsible for the excitation of annual- and semiannual propagating Rossby waves in the eastern sub-basin

Hunt et al., Ocean Sci, 2012

Argo profiling floats provide a hope of a widespread method for detecting the structure of Rossby waves below the surface. Chu et al. (2007) used data from Argo floats in the North Atlantic to extract vertical profiles of Rossby waves. They found that the second baroclinic mode was always dominant, with the contributions of other modes geographically variable. This produced profiles with a subsurface maximum at approximately 1000 m and a secondary maximum in the region of 100 m with no reversal at depth, in concurrence with the results of Hagen (2005).

Overall these studies support Chelton and Schlax (1996)'s conclusions that the standard linear theory for Rossby waves is inadequate to account for the properties of actual signals

Conclusions

- OSD is a useful method especially for ocean data assimilation. No background error covariance matrix B is needed.
- OSD method effectively uses the ocean topography and lateral boundary conditions.
- The basis functions are orthonormal
- The basis functions are the eigen functions of the Laplacian operator (pre-determined).